Title:

Flattened circadian glucocorticoid oscillations cause obesity due to increased lipid turnover and lipid uptake

Authors: Stefan Tholen[1], Kyle Kovary[1], Atefeh Rabiee[1], Ewa Bielczyk-Maczyńska[1], Wenting Yang[1] and Mary N. Teruel[1,*]

Affiliations:
[1]Department of Chemical and Systems Biology, Stanford University, Stanford, CA, 94305, USA.

[*]**Corresponding Author and Lead Contact:** mteruel@stanford.edu

ABSTRACT

Chronic stressors flatten circadian glucocorticoid oscillations, which has been correlated with negative health outcomes including obesity. How flatter circadian glucocorticoid oscillations affect metabolism and fat storage remains unknown. Here we aimed to investigate the consequences of flattened glucocorticoid oscillations in mice. We found that flattening glucocorticoid oscillations not only results in body weight gain mainly due to an increase in white fat depot mass, but also leads to fat accumulation in brown adipose tissue and to hyperinsulinemia. A transcriptomic analysis of white and brown adipose tissues revealed that flattened glucocorticoid oscillations resulted in a dysregulated lipid metabolism with a prominent role of Cd36. Indeed, Cd36 knockout mice are partially protected against body weight gain and lipid accumulation in the brown and visceral white fat depots induced by flattened glucocorticoid oscillations. These results provide insights how conditions associated with flattened glucocorticoid levels cause obesity.

KEYWORDS

Obesity, stress, circadian rhythm, hormone oscillations, glucocorticoids, brown adipose tissue, white adipose tissue, lipid metabolism, Cd36

HIGHLIGHTS

- Flattening of circadian glucocorticoid oscillations in mice results in body weight gain, lipid accumulation in white and brown adipose tissue, and hyperinsulinemia.
- Transcriptomic analysis of BAT and WAT revealed gene expression alterations pointing to dysregulated lipid metabolism caused by flattened glucocorticoid oscillations, including upregulation of Cd36.
- Cd36ko mice are partially protected against body weight gain and lipid accumulation in brown adipose tissue and visceral fat upon flattening glucocorticoid oscillations.

INTRODUCTION

In healthy mammals glucocorticoids (GCs) are secreted in circadian oscillations that are low during sleep and peak before awakening to prepare the body for its metabolic needs (Weitzman et al., 1971). Synthetic GCs are widely used for medical treatment for their anti-inflammatory and immune suppressive properties. Long-term treatment with GCs has been shown to cause side effects including obesity, dyslipidemia, insulin resistance, hyperinsulinemia, and diabetes (Hoes et al., 2011; Schäcke et al., 2002). Some of these side effects are caused by the major role GCs have in adipocyte biology affecting adipogenesis (Hauner et al., 1987; Rosen and MacDougald, 2006), lipogenesis and lipolysis (Lee et al., 2014; Peckett et al., 2011) as well as thermogenesis (Ramage et al., 2016; Strack et al., 1995; Van Den Beukel et al., 2014).

Circadian secretion of GCs is strongly controlled by the hypothalamic-pituitary-adrenal (HPA) - axis, which responds strongly to stress. GCs are secreted in response to both acute stress ("fight or flight" response) and chronic stress. A chronic stress state can result in flatter diurnal glucocorticoid oscillations, which are characterized by an elevation of trough GC levels and a decrease in the peak GC levels, but without a significant increase in daily mean values (Adam, 2017; Dallman et al., 2000). A growing body of evidence suggests that these changes in GC rhythms, and not only excessive amounts of GCs, play a significant role in human health and disease. Depression, jet lag, irregular eating and sleeping cycles, aging, or prolonged treatment with GCs can all result in flattened GC oscillations and have been shown to closely correlate with obesity (Adam, 2017; Broussard and Cauter, 2016; Dallman et al., 2000; Doane et al., 2013).

In our previous work, we uncovered the mechanisms by which loss of the daily circadian oscillation pattern of GCs leads to increased adipogenesis, providing a molecular explanation for why chronic stress and other conditions in which GC oscillations are flattened may lead to obesity (Bahrami-Nejad et al., 2018). In particular, we demonstrated that preadipocytes failed to differentiate in vitro in response to short or pulsatile GC stimuli of 12-hour peak duration whereas more persistent GC signals triggered fat cell differentiation. We showed that this differentiation decision is controlled

by a filtering mechanism requiring a slow and fast positive feedback circuit that controls PPARG, the main regulator of adipogenesis. In addition, we found that flattening circadian GC oscillations results in body weight gain and expansion of the white fat depots.

In this study we now provide a time course analysis of this process, showing that the white fat depots already accumulate lipids after 7 days of flattening GC oscillations in mice. Furthermore, we identified the expansion of the white fat depots as the major contributor to body weight gain since the white fat depots expanded 2-3 fold. In addition, we show for the first time that flattening of GC oscillations leads to hyperinsulinemia as well as lipid accumulation in brown adipose tissue (BAT), which precedes expansion of the white adipose tissue (WAT). Analysis of the transcriptome of WAT and BAT revealed alterations in gene expression dependent on flattened GC oscillations and pointed to increased lipid turnover and lipid uptake in both fat depots finally resulting in lipid accumulation in BAT and WAT. The fatty acid transporter Cd36 was upregulated in WAT and BAT upon flattening of GC oscillations. The importance of Cd36 for lipid accumulation was highlighted by using Cd36 knockout mice, which were partially protected against body weight gain, and lipid accumulation in visceral WAT and BAT induced by flattening of GC oscillations.

RESULTS

Flattening of daily corticosterone oscillations in mice results in lipid accumulation in white adipose tissue

Previous studies showed that increased glucocorticoid levels promote the development of obesity (Lee et al., 2014; Peckett et al., 2011). Unfortunately most of these in vivo studies involve administration of high glucocorticoid concentrations which does not provide insight into how physiological variations in systemic glucocorticoid levels throughout the day affect the body (Lee et al., 2014). To investigate the effect of flattening daily glucocorticoid levels, as seen during chronic stress (Adam, 2017; Lightman and Terry, 2014; Miller et al., 2007), on adipose tissue, we implanted corticosterone pellets

subcutaneously in C57BL/6J male mice. The corticosterone dose released by the corticosterone pellet per day was chosen based on previous studies to just flatten normal daily corticosterone levels while keeping mean corticosterone levels within normal physiological levels **(Fig. 1A)** (Bahrami-Nejad et al., 2018; Hodes et al., 2012). Hence, mice implanted with corticosterone pellets showed increased corticosterone levels in the nadir of the diurnal corticosterone pattern and decreased corticosterone at the peak time in the evening compared to sham pellet implanted mice.

Confirming the results of our previous study (Bahrami-Nejad et al., 2018), mice with flattened corticosterone oscillations increased their body weight faster than sham pellet implanted mice and ended up weighing 9.1% more after 21 days **(Fig. 1B)**. Interestingly, as has been found in other studies in which sustained GCs were given long-term (Bowles et al., 2015; Luijten et al., 2019a), the increased weight gain cannot be explained by higher food intake **(Fig. 1C)**, and a reduction in metabolism may be a more significant contributing factor. To test whether corticosterone pellet implanted mice gain weight mainly by expansion of the white fat depots, the subcutaneous inguinal WAT and the visceral epididymal WAT were dissected and weighed. The inguinal and epididymal are the main fat pads, with the latter being the most frequent dissected fat pad (Chusyd et al., 2016). Located under the skin the inguinal WAT is part of the subcutaneous WAT (sWAT) and we will refer to it as sWAT. The epididymal WAT represents the major visceral WAT (vWAT), and we will refer to it as vWAT throughout this study. In general, a stronger expansion was observed for the vWAT, which expanded 3-fold in 21 days. The weight of the sWAT increased slightly more than 2-fold. Both white fat depots showed a significant increase in organ weight already 7 days of flattening corticosterone oscillations **(Fig. 1D-G)**. This early expansion of the white fat depots was confirmed by hematoxylin and eosin (H&E) staining of sWAT and vWAT revealing increased cell volume of the adipocytes in both fat depots from day 7 **(Fig. 1H/J)**, which was quantified in **Figures 1I/K**.

Increasing the peak amplitudes of corticosterone does not result in lipid accumulation in the white fat depots

To test whether that lipid accumulation in the white fat depots as described in Figure 1 is due to flattening of diurnal corticosterone levels and not caused by the amount of corticosterone released by the corticosterone pellet, we injected the same amount that is released by the corticosterone pellet per day as one single subcutaneous injection in the evening (17:00) for 21 days. This injection resulted in a more than 10-fold increase in the daily peak amplitude of corticosterone **(Fig. 2A)**. Strikingly, corticosterone-injected mice did not show a significant increase in body weight compared to sham-injected control mice **(Fig. 2B)** which could be expected since food intake was not altered **(Fig. 2C).** In addition, no differences in fat pad weight were detected between the sWAT **(Fig. 2D/E)** and vWAT of the corticosterone- and sham-injected mice **(Fig. 2G/H)**, and histological analysis of the tissues showed no differences in lipid accumulation **(Fig. 2F/I)**.

In conclusion, increasing the peak amplitude of corticosterone in the evening phase did not affect body weight gain or lipid accumulation in the white fat depots. Hence short spurts of glucocorticoids do not seem to promote weight gain as long as the increase in glucocorticoids occurs during a short time window and leaves sufficiently long off-periods with low glucocorticoid levels (Dallman et al., 2000)). The fact that corticosterone pellet implanted mice and corticosterone injected mice received the same concentration of corticosterone per day and only the pattern of the diurnal corticosterone levels as measured in blood serum differed **(Fig. 1A/2A)**, showed that flattening of diurnal corticosterone levels resulted in body weight gain and was responsible for lipid accumulation in the white fat depots **(Fig. 1)**.

Flattening of daily corticosterone oscillations in mice results in lipid accumulation in brown adipose tissue (BAT)

BAT is a specialized organ that is using carbohydrates and fat as a resource to produce thermal energy to regulate body temperature (Cannon and Nedergaard, 2004). In rodents, BAT has shown to be protective against metabolic disease and obesity (Feldmann et al., 2009). With the discovery of thermogenic brown adipocytes in humans (Cypess et al., 2009; Saito et al., 2009; Van Marken

Lichtenbelt et al., 2009), BAT expansion or boosting its respiratory activity gained significant attention as a therapeutic treatment for obesity and related disorders (Betz and Enerbäck, 2015; Harms and Seale, 2013; Kusminski et al., 2016; Sidossis and Kajimura, 2015). Numerous studies showed that GC treatment in rodents can lead to accumulation of lipids in the brown fat depot (Ketzer et al., 2019; Luijten et al., 2019a; Shen et al., 2017; Strack et al., 1995). To test if flattening of diurnal corticosterone oscillations without increasing the total corticosterone amount per day is already sufficient to cause lipid accumulation, we analyzed BAT of corticosterone and sham pellet implanted mice. Indeed, flattening diurnal corticosterone oscillations resulted in an increase in BAT size **(Fig. 3A)** and a 3-fold increase in organ weight **(Fig. 3B)**. This was confirmed by histological analysis of BAT, where larger lipid-filled adipocytes could be detected. **(Fig. 3C**, quantified in **Fig. 3D)**. The lipid droplets were characterized by a shift from a multilocular to a more unilocular morphology, giving the tissue a "whitened" appearance. As observed for the white fat depots, injection of the same corticosterone amount released by the corticosterone pellet per day increased the peak amplitude in the evening/waking phase, bit did not affect tissue size **(Fig. 3E/F)**. In line with this observation, histological analysis of BAT did not reveal any morphological changes comparing mice subcutaneously injected with corticosterone to mice injected with the solvent control **(Fig. 3G)**. As shown for WAT, the daily dose of corticosterone given to the mice did not cause lipid accumulation in the fat tissue. Rather the flattening in the diurnal pattern of corticosterone oscillations is promoting fat deposition in WAT and BAT. Interestingly lipid accumulation in BAT was already detected 3 days after corticosterone pellet implantation preceding lipid accumulation in subcutaneous and visceral WAT, which was first detected 7 days after pellet implantation **(Fig. 1E/G)**. In conclusion, BAT reacts more sensitively to flattening of corticosterone oscillations than the white fat depots analyzed in this study.

Flattening of daily corticosterone oscillations in mice does not result in hyperlipidemia or fat deposition in the liver

Rodents treated with chronic high concentrations of corticosterone have been shown to rapidly increase body weight due to expansion of the fat depots (Bowles et al., 2015; Campbell et al., 2011; Chimin et al., 2014; Karatsoreos et al., 2010). Often the expansion of fat depots is accompanied by fat deposition in the liver, an increase of triglycerides in blood plasma, and insulin resistance (Bowles et al., 2015; Campbell et al., 2011; Chimin et al., 2014; Karatsoreos et al., 2010). Since we detected an expansion of WAT and BAT induced by flattening of corticosterone, we wanted to test if these parameters are also affected by flattening of corticosterone oscillations.

To test if flattening of corticosterone oscillations leads to fat deposition in the liver, we performed a histological analysis of the liver of sham and corticosterone pellet implanted mice. We did not detect fat deposition in the liver upon flattening of corticosterone oscillations (**Fig. 4A**) and the organ weight of the liver remained unchanged over the treatment period of 21 days (**Fig. 4B**). Also increasing the peak amplitude in the evening phase by injection of corticosterone with the same amount the corticosterone pellet releases per day did not lead to fat deposition in the liver (**Fig. 4A/C**). In line, no significant gene expression alterations were detected for a number of genes involved in lipid deposition upon flattening corticosterone oscillations or increasing the peak amplitude. The analyzed genes include the fatty acid transporter Cd36, Hsd11b1, Pepck, Angptl4, and the lipolytic genes Lipe (HSL) and Atgl (**Sup. Fig. 1**). A non-significant increase in gene expression was observed for Fasn, Dgat2, Srebp1c, and Glut4 in corticosterone pellet implanted and corticosterone injected mice. As these changes in gene expression are discovered with both corticosterone treatments, they seem to be caused by the total amount of corticosterone given to both mouse models per day and were not exclusively caused by flattening of corticosterone levels (**Sup. Fig. 1**).

Furthermore, we assessed if flattening of corticosterone oscillations increases triglycerides circulating in the blood. We determined the levels of total triglycerides as well as glycerol and free fatty acids (FFA), which are the building blocks of triglycerides, in blood serum. We did not detect a difference between mice implanted with sham and corticosterone pellets (**Fig. 4D-F**). Although we detected a minor significant difference in glycerol, FFA, and triglycerides comparing sham and

corticosterone pellet implanted mice at day 14, this effect seems unlikely to be relevant, because levels of glycerol, FFA, and triglycerides in corticosterone pellet implanted mice did not increase over time. At the same time sham pellet implanted control mice decreased glycerol, FFA, and triglyceride levels, which resulted in the described effect and can be explained due to variation between sham pellet implanted mice. No increase in triglyceride, glycerol, and FFA levels was detected when the peak amplitude of corticosterone was increased in the evening phase (**Fig. 4G-I**).

Flattening of daily corticosterone oscillations in mice causes hyperinsulinemia

To assess the effect of flattening of corticosterone oscillations on glucose metabolism, we performed glucose tolerance tests (GTT) and insulin tolerance tests (ITT). Initially mice implanted with corticosterone pellets seemed to be more insulin-sensitive as measured in blood plasma after intraperitoneal injection of glucose (**Fig. 5A**). In contrast, results from the ITT pointed to these mice being insulin-resistant (**Fig. 5B**). Determination of insulin concentrations in blood plasma taken during the GTT revealed 3-fold higher insulin levels in pellet implanted mice explaining the discrepancy between the GTT and ITT (**Fig. 5A**). In conclusion, mice with flattened corticosterone levels remained glucose tolerant, but developed hyperinsulinemia. Mice injected with the same dose of corticosterone that was released by the pellet per day did not reveal any differences in glucose tolerance compared to sham injected mice and did not display higher insulin levels in the blood plasma (**Fig. 5C/D**), demonstrating the flattening of the diurnal corticosterone pattern to be responsible for the increased insulin levels.

To determine when insulin levels increase we performed a time course analysis monitoring insulin levels in blood plasma over 21 days in corticosterone and sham pellet implanted mice. We found that insulin levels are more than 7-fold increased already at day 3 after flattening of corticosterone oscillations. This increase slowly decreases during the 21-day time course, but is still 3-fold higher at day 21 (**Fig. 5E**). High insulin levels resulted in reduced blood glucose levels (**Fig. 5F**). Interestingly, flattening of corticosterone oscillations induced hyperinsulinemia already before

expansion of the white fat depots and might even contribute to their expansion. A summary of all parameters measured in mice upon different treatments can be found in **Supplementary Table 1**.

Transcriptomic analysis of vWAT reveals gene expression alterations upon flattening of corticosterone oscillations

To elucidate how gene expression is globally affected by flattening of glucocorticoid oscillations and finally affecting expansion of the fat depots, we performed RNAseq analysis of vWAT. Analysis of vWAT was chosen since its expansion has been recognized to be detrimental to metabolic health, while accumulation of sWAT may be protective. For RNAseq analysis mice were subcutaneously implanted with corticosterone pellets to flatten their corticosterone oscillations and the vWAT was harvested 0, 3, 7, and 14 days after pellet implantation. These time points were chosen based on the time point when expansion of BAT or WAT was observed for the first time. Notably, most differently expressed genes in vWAT already displayed alterations in gene expression 3 days after flattening corticosterone oscillations, before expansion of WAT was detected. In **Figure 6A** it is nicely demonstrated that the observed alterations in gene expression cluster by the type of treatment and not by length of pellet implantation. Based on this result and with the goal to increase significance and accuracy of our data we disregarded the length of treatment for subsequent analysis. In total we found 708 genes differently expressed comparing corticosterone and sham pellet implanted mice (cutoff criteria: fold change of 1.5 and p value < 0.05; days 3-14 were combined for analysis). Of these 359 genes were upregulated and 349 were downregulated (**Sup. Table 2**).

To control that these changes in gene expression are due to flattening of diurnal corticosterone oscillations and not caused by the amount of corticosterone released by the corticosterone pellet, a similar RNAseq analysis was performed comparing corticosterone and sham injected mice. As mentioned before, these mice were injected with the same amount of corticosterone released by the corticosterone pellet per day in one single injection, thereby increasing the peak amplitude of corticosterone in the evening phase. In this comparison, no alterations in gene expression were

identified based on the above-mentioned cutoff criteria. In line with this finding, no clustering of the data was observed based on differently expressed genes between the different treatment groups or length of treatment (**Sup. Fig. 2A**). In conclusion, the comparatively low dose of corticosterone increasing the peak amplitude of corticosterone in the evening phase did not affect gene expression, but flattening of corticosterone oscillations did.

Flattening of corticosterone oscillations affects expression of metabolic enzymes in vWAT

To obtain a global picture of pathways and gene classes affected in our transcriptomic data comparing vWAT of sham and corticosterone pellet implanted mice, we performed gene ontology (GO) analysis. As expected regarding the use of glucocorticoids as immune suppressants, the top categories identified were related to different aspects of immune function, making up 66% of all enriched GO terms (**Fig. 6B; Sup. Table 3**). Interestingly, the second most category of enriched GO terms were metabolism related (15%). Keeping in mind the strong expansion of the white fat depots, we focused on this category, which combined GO terms mostly related to glucose and lipid metabolism (**Fig. 6C**). Especially glycolytic genes, including the rate limiting enzymes Pfkl and Pkm, and genes promoting glycolysis were upregulated. (**Fig. 6D**). Upregulation of the glycolytic genes could result in increased production of pyruvate, which will be further converted to Acetyl-CoA by the pyruvate dehydrogenase complex. Components and activators of the pyruvate dehydrogenase complex were upregulated as well, including Pdha1, Dlat, and Pdk4. This process possibly promotes the conversion of carbohydrates into fatty acids and might significantly contribute to lipid accumulation in the vWAT upon flattening of corticosterone oscillations.

Glucocorticoids have been shown to simultaneously increase pathways of triglyceride (TG) synthesis and breakdown (Lee et al., 2014; Peckett et al., 2011). Interestingly, flattening of daily corticosterone oscillations in mice could result in a similar situation as it induces expression of genes involved in de novo lipogenesis, including the key enzymes fatty acid synthase (Fasn) and Acetyl-CoA carboxylase (Acaca), and genes involved in lipolysis, including the rate limiting enzyme Pnpla2 (Atgl)

(Haemmerle et al., 2006) (**Fig. 6D**). In addition, we observed upregulation of several other genes controlling TG homeostasis, e.g. Scd1, Scd2, Lpgat1, Acadm and the fatty acid transporter Cd36 (**Fig. 6D; Sup. Table 2**). Flattening of corticosterone oscillations alters expression levels of these genes and possibly tips the balance of lipid synthesis and breakdown towards fat accumulation. Of interest to the gene expression alterations observed for metabolic enzymes, core components of the circadian clock as well as regulators of the circadian rhythm were altered. These include Clock, Arntl/Bmal1, and Per3 (**Fig. 6C/D; Sup. Table 2**). The circadian clock coordinates the timing and activity of enzymes involved in TG synthesis and breakdown (Lekkas and Paschos, 2019). For example the circadian clock is found to control Atgl and Scd1 (Paschos et al., 2013; Shostak et al., 2013).

vWAT and BAT show differences and common features in gene expression profiles upon flattening of corticosterone oscillations

To elucidate how flattening of corticosterone oscillations affects gene expression globally in BAT and if similar processes are responsible for lipid accumulation in BAT and vWAT, we performed RNAseq analysis of BAT. As for the transcriptomic analysis of vWAT, mice were subcutaneously implanted with corticosterone pellets to flatten their corticosterone oscillations and BAT was harvested 0, 3, 7, and 14 days after pellet implantation. Like in vWAT (**Fig. 6A**), most differently expressed genes cluster by the type of treatment and not by length of pellet implantation, showing most gene expression alterations already on day 3 (**Fig. 7A**). Based on this observation and with the goal to increase significance and accuracy of our data we disregarded the length of treatment for subsequent analysis like done before for the analysis of vWAT. In total we found 1686 genes differently expressed comparing BAT of corticosterone and sham pellet implanted mice (cutoff criteria: fold change of 1.5 and p value < 0.05; days 3-14 were combined for analysis). Of these, 601 genes were upregulated, and 1085 genes were downregulated (**Sup. Table 4**). 296 genes were found to be differently expressed in BAT and vWAT.

To control that gene expression alterations in BAT are due to flattening of diurnal corticosterone oscillations and not caused by the amount of corticosterone released by the corticosterone pellet, RNAseq analysis was also performed comparing BAT of corticosterone and sham injected mice. No clustering of the data was observed based on differently expressed genes between the different treatment groups or length of treatment (**Sup. Fig. 2B**). Only Abcd2 (FC = 1.8; p = 0.01) was differently expressed in BAT upon corticosterone injection. In conclusion, all other differently expressed genes identified in BAT upon corticosterone pellet implantation are caused by flattening of corticosterone oscillations.

We performed GO analysis and found mostly GO terms related to immune response ranked in the top categories (**Fig. 7B; Sup. Table 5**). Immune response related GO terms accounted for 57% of all GO terms ($p < 0.01$) in BAT, which was similar in vWAT (66%; **Fig. 6B**). Interestingly, the second most ranked category of enriched GO terms in BAT was ion transport/homeostasis related (14%), which was not observed in vWAT. Furthermore, metabolism related GO terms, forming a bigger class in vWAT, were not that relevant in BAT. For example, GO terms related to glycolysis were missing in the analysis of BAT (**Fig. 7C/ Sup. Table 5**). In line, most glycolytic genes upregulated in vWAT were not differently expressed in BAT (**Fig. 7D**).

A dysregulation of lipid metabolism, as seen for vWAT, can also be assumed in BAT. Numerous genes involved in TG synthesis and degradation as well as their regulators were differently expressed in both fat depots (**Fig. 7D**). These include Acaca, Pnpla2 (Atgl), Scd1, Cd36, leptin, and HSD11ß1. Although Fasn was not differently expressed in BAT, gene expression of other genes controlling fat metabolism were exclusively altered in BAT. Lpin1, which is important during TG synthesis, was upregulated in BAT as well as Acsm5, which catalyzes the production of acyl-CoA, the first step of fatty acid metabolism. As observed in vWAT, flattening of corticosterone oscillations in BAT alters expression levels of genes in lipid metabolism and thereby promotes lipid accumulation. Here also the circadian clock, as a circadian regulator of lipid metabolism, might play a major role,

because alterations in gene expression of core clock components (Clock, Arntl, Per3) were observed in BAT (**Fig. 7D**).

Flattening of corticosterone oscillations affects regulators of BAT activity including UCP1

Upon activation of the sympathic nervous system, e.g. in response to cold exposure, BAT produces heat through activation of mitochondrial uncoupling protein 1 (UCP1) that releases energy generated by mitochondrial respiration as heat instead of being used for ATP production (Cannon and Nedergaard, 2004). Because of this energy expenditure fueled by the breakdown of TGs, activation of BAT is considered an attractive approach to prevent obesity (Liu et al., 2012; Strack et al., 1995; Van Den Beukel et al., 2014). Interestingly, Ucp1 expression decreases more than twofold upon flattening of corticosterone oscillations (FC = -1.1; p = 0.001; **Sup. Table 4**), which was confirmed by qPCR (**Fig. 7E**). GO analysis of the RNAseq data of BAT revealed GO terms changed that are associated with temperature control (**Fig. 7C**) and pointed to downregulation of additional regulators of BAT differentiation and activity, including Cidea (FC = -0.7; p = 0.001) and Elovl3 (FC = -1.4; p = 0.011). Furthermore the Ucp1-activator Pgc1a was decreased (**Fig. 7E**). In conclusion, we found numerous regulators of BAT activity, including Ucp1, downregulated upon flattening of corticosterone oscillations. Based on this observation, we hypothesized that lower BAT activity contributes to lipid accumulation in BAT and might result in defective non-shivering thermogenesis upon flattening of corticosterone oscillations. We performed acute cold exposure experiments measuring the core body temperature of sham and corticosterone pellet implanted mice for 6 hours at 6°C. No difference was observed between both treatment groups suggesting that flattening of corticosterone oscillations in mice does not affect non-shivering thermogenesis (**Sup. Fig. 3**).

CD36ko mice are partially protected against weight gain induced by flattening of corticosterone oscillations

The transcriptomic analysis identified upregulation of Cd36 upon flattening of corticosterone oscillations a common feature between WAT and BAT (**Fig. 6D/7D**). To elucidate if Cd36 contributes to lipid accumulation in WAT and BAT, we first wanted to validate this data. QPCR of vWAT and BAT confirmed 3-fold higher mRNA levels in vWAT and 1.5-fold higher mRNA levels in BAT upon flattening of corticosterone oscillations (**Fig. 8A**). To investigate the role of Cd36 in lipid accumulation upon flattening of corticosterone oscillations in vivo, we implanted sham and corticosterone pellets in Cd36ko mice and monitored their body weight for 21 days (Febbraio et al., 1999). After 21 days, corticosterone pellet implanted Cd36ko mice weighed 6.9% more than sham implanted Cd36ko mice, which is 2.2% less than observed in wild-type mice (**Fig. 8B**). In wild-type mice, corticosterone pellet implanted mice weighed 9.1% more than sham implanted mice (**Fig. 1B/8B**). In conclusion, Cd36ko mice are partially protected against body weight gain induced by flattening of corticosterone oscillations. Of note, during the experiment Cd36ko gained less weight compared to wild-type mice (3.2% less comparing sham pellet implanted mice and 5.4% less comparing corticosterone pellet implanted mice). Furthermore corticosterone pellet implanted Cd36ko mice started to gain weight 2 days later than corticosterone pellet implanted wild-type mice.

To determine if the lower body weight gain of corticosterone implanted Cd36ko mice is manifested in lower organ weights of the white fat depots, sWAT and vWAT were dissected and weighed. Strikingly, vWAT of corticosterone pellet implanted Cd36ko mice increased weight in average by only 208mg, which is significantly less than vWAT of wild-type mice (801mg) (**Fig. 1G/8C**). Histological analysis of vWAT corroborated the protective effect of Cd36 against expansion of vWAT (**Fig. 8D**). Epididymal adipocytes of corticosterone pellet implanted Cd36ko mice displayed lower increase in cell volume than corticosterone pellet implanted wild-type mice (**Fig. 8E**). Surprisingly, no significant difference was observed in increase of organ weight of sWAT between corticosterone pellet implanted Cd36ko and wild-type mice (**Fig. 8F**). The weight of the sWAT increased 2-fold comparing sham and corticosterone pellet implanted Cd36ko mice, which was also observed for wild-type mice (**Fig. 1E**). In addition, no difference in cell volume of the adipocytes was observed (**Fig. 8G/H**). In

conclusion, Cd36 partially protects vWAT from lipid accumulation induced by flattening of corticosterone oscillations. This protective effect is not observed for sWAT, pointing to depot-specific differences between the visceral and subcutaneous fat depot.

A protective role of Cd36 against lipid accumulation induced by flattening of corticosterone oscillations was also observed in BAT. As observed for vWAT, BAT of corticosterone pellet implanted Cd36ko mice expanded less compared to corticosterone pellet implanted wild-type mice (**Fig. 8I**). This was substantiated by histological analysis of BAT showing less lipid accumulation and lower cell volume of brown adipocytes in Cd36ko mice compared to wild-type mice upon flattening of corticosterone oscillations (**Fig. 8J/K**).Although a protective role for Cd36 against body weight gain and expansion of vWAT and BAT upon flattening corticosterone oscillations was detected, Cd36 did not protect against hyperinsulinemia. Insulin levels even increased in corticosterone pellet implanted Cd36ko mice comparing them to corticosterone pellet implanted wild-type mice (**Sup. Fig. 4A**). In line and as observed in wild-type mice, corticosterone pellet implantation in Cd36ko mice resulted in lower blood glucose levels (**Sup. Fig. 4B**). Interestingly, higher insulin levels were also observed comparing sham pellet implanted Cd36ko mice and sham pellet implanted wild-type mice, suggesting that Cd36ko mice show in general higher insulin levels (**Sup. Fig. 4A**).

DISCUSSION

In this study we investigated explicitly the consequences of flattening glucocorticoid oscillations, which occurs during chronic stress and is associated with depression, fatigue, cardiovascular disease, and mortality of cancer patients (Adam, 2017; Doane et al., 2013; Kumari et al., 2009; Matthews et al., 2006; Sephton et al., 2013). We show that flattening of circadian glucocorticoid oscillations in mice, while keeping the overall glucocorticoid concentrations the same during the day, results in body weight gain, expansion of the white and brown fat depots and hyperinsulinemia. All these pathologies were not observed when the peak amplitude was increased in the evening phase by injection of corticosterone, showing that as long as glucocorticoid increases are

restricted to the normal peak time period, they cause no / less weight gain. Flattening of glucocorticoids, as done in this study, results in elevation in trough concentrations and is accompanied by a reduction in peak concentrations with no change in the daily mean values. Such loss of trough or "off periods" has been shown to increase body weight and expansion of the fat depots (Bahrami-Nejad et al., 2018; Dallman et al., 2000). The duration of the "off-periods" was also shown to be important in our previous study focusing on adipogenesis (Bahrami-Nejad et al., 2018). We demonstrated that preadipocytes fail to differentiate in vitro in response to 12hr on / 12hr off pulses of glucocorticoid stimuli simulating circadian glucocorticoid secretion due to a filtering mechanism requiring a slow and fast positive feedback circuit that controls PPARG. Shortening the "off" periods by extension of the glucocorticoid pulses beyond normal circadian pulse durations increased the fraction of differentiated cells (Bahrami-Nejad et al., 2018).

Glucocorticoids exhibit pleiotropic effects on lipid metabolism simultaneously promoting lipolysis and lipid synthesis as well as increasing adipogenesis (for review, see (Lee et al., 2014, 2018; Peckett et al., 2011)). In this study we aimed to elucidate gene expression changes directly dependent on flattened diurnal glucocorticoid oscillations with keeping the normal daily mean values of glucocorticoids. In this regard our study is different from many other studies performed in recent years, because we just flatten glucocorticoid levels without using high concentrations. To identify genes induced by flattening of glucocorticoids we performed RNAseq analysis of vWAT and BAT. Surprisingly, we observed similar expression alterations upon flattening of glucocorticoids as already described for application of glucocorticoids in higher concentrations, showing that chronic stress conditions could cause effects similar to side effects during glucocorticoid medication. In vWAT we found genes involved in TG synthesis (e.g. Fasn, Acaca, Scd1, Scd2, Lpin1) lipid uptake (e.g. Cd36), and lipolysis (e.g. Pnpla2/Atgl) affected, indicating that flattening of glucocorticoids results in increased lipid turnover. Interestingly, functional GR binding sites have been identified for Acaca, Fasn, Scd1, Scd2, Lpin1, and Cd36 (Yu et al., 2010).

Nevertheless, not all genes known to exhibit functional GR binding sites were differently

expressed in our study. For example, Angptl4 has been shown to be regulated by glucocorticoids through a glucocorticoid response element (GRE) (Koliwad et al., 2009). Angptl4 inhibits the activity of extracellular lipoprotein lipase (LPL), which is important for FFA uptake and induces lipolysis in adipocytes resulting in overall increase in plasma TG levels (Gray et al., 2012). Although a glucocorticoid binding region (GBR) for Lpl was also identified in 3T3-L1 adipocytes (Yu et al., 2010), upregulation of Angptl4 and Lpl was not observed in the RNAseq of vWAT or BAT upon flattening of glucocorticoids. No change in gene expression was validated for Angptl4 and Lpl by qPCR in BAT (data not shown). Furthermore no difference in Angptl4 expression was found in liver comparing sham and corticosterone pellet implanted mice (**Sup. Fig 1J**) and increased levels of TG were not detected in blood plasma (**Fig. 4D/E/F**). This exemplifies that not all processes normally induced by high temporal doses of glucocorticoids are also influenced by flattening of glucocorticoids. This observation leads to the hypothesis if adipocytes exhibit specific factors only induced upon flattening of glucocorticoid that guide the specific glucocorticoid-response induced by flattening. The existence of such factors would maybe also explain tissue-specific differences in the response to flattening and maybe explain why glycolysis or Fasn expression is only affected in vWAT and not BAT. However, existence of such factors needs further investigation.

As a therapeutic treatment for obesity and related disorders, expansion of BAT, or boosting its respiratory activity with the goal to increase energy expenditure, has gained significant attention (Bartelt et al., 2011; Feldmann et al., 2009; Saito, 2013). However, how BAT is controlled by the pattern of circadian glucocorticoid oscillations has hardly been investigated and could impact therapeutic strategy. Lipid accumulation in BAT upon glucocorticoid treatment has been reported previously (Ketzer et al., 2019; Luijten et al., 2019a; Shen et al., 2017; Strack et al., 1995), but here we show for the first time that flattening of daily corticosterone oscillations in mice leads to lipid accumulation in BAT as well. We hypothesized that this could impact the functionality of the tissue. This assumption was further supported when we found numerous regulators of thermogenesis, including Ucp1, downregulated. Surprisingly, acute cold exposure experiments in mice did not show differences in

thermogenesis, which leads to the question how strong downregulation of Ucp1 upon flattening of glucocorticoids actually contributes to lipid accumulation in adipose tissue. It was recently demonstrated that the development of glucocorticoid-induced obesity is not caused by a decreased UCP1-dependent thermogenic capacity (Luijten et al., 2019a). The contribution of UCP1 in causing metabolic effects upon glucocorticoid treatment is maybe overestimated due to experimental design of previous studies (for review: (Luijten et al., 2019b)). However, in this study reduced energy expenditure due to downregulation of Ucp1 does not or only play a minor role in promoting lipid accumulation in BAT. It rather seems that flattening of glucocorticoid oscillations dysregulates lipid metabolism resulting in a futile cycle of TG synthesis and breakdown finally causing lipid storage. This would be a similar situation as described for WAT and is supported by gene expression alterations observed for Acaca, Pnpla2 (Atgl), Scd1, Cd36, leptin, Hsd11ß1, and additional metabolic enzymes in both fat depots.

A common feature between lipid accumulation in BAT and vWAT induced by flattening of corticosterone oscillations is the strong upregulation of Cd36. Cd36 has been shown to facilitate fatty acid uptake into muscles and adipose tissue in rodents and humans (Abumrad et al., 1993; Glatz et al., 2010). Since several studies demonstrated that Cd36 deficiency protects against high fat diet induced obesity (Hajri et al., 2007; Koonen et al., 2010; Vroegrijk et al., 2013), we hypothesized that knocking out Cd36 might protect against weight gain induced by flattening of glucocorticoids as well. Indeed we found that Cd36ko mice are partially protected against body weight gain and lipid accumulation in vWAT and BAT. This can likely be explained by its role in fatty acid intake, but also additional aspects of Cd36 functionality related to fatty acid metabolism including fat taste perception, fat absorption, and fat utilization cannot be excluded (review: (Pepino et al., 2014)).

It has been reported that BAT of mice lacking Cd36 display a whitened phenotype and increased lipid droplet size (Anderson et al., 2015). However, in the current study we did not detect differences in BAT weight or lipid droplet size between sham pellet implanted Cd36ko and wild-type mice, which might also be explained by the fact that younger mice were used in this study, which had

less time to accumulate fat. Although Cd36ko did not prevent hyperinsulinemia upon flattening of corticosterone oscillations, we observed higher insulin levels in Cd36ko versus wild-type mice implanted with sham pellets. Furthermore we found a trend towards lower plasma glucose levels in Cd36ko mice, which was reported before in Cd36ko mice (Febbraio et al., 1999) and using a Cd36 inhibitor in mice (Yang et al., 2018). This suggests that metabolic actions of Cd36 are more complex and cannot be reduced to its role as a fatty acid transporter. Cd36 deficiency has been shown to affect insulin signaling (Samovski et al., 2018) and to generate intracellular PPARG ligands which will activate PPARG signaling (Nagy et al., 1998; Tontonoz et al., 1998). By being highly expressed in immune cells and adipocytes Cd36 has been implicated in the development of insulin resistance and diabetes. The soluble form of Cd36 circulating in the blood plasma has been identified as a novel marker of insulin resistance in diabetes (Alkhatatbeh et al., 2013; Handberg et al., 2010). These findings suggest Cd36 as a potential target for intervention of metabolic disorders associated with obesity.

The data presented in this study identified consequences of flattening of glucocorticoids such as is observed during chronic stress. It underlines that small alterations or losing the normal diurnal glucocorticoid oscillation pattern can result in obesity. Similar to clinical treatments with higher glucocorticoid concentrations, flattening of glucocorticoids has pleiotropic effects on gene expression in a multiplicity of organ systems, including BAT and WAT. In line, knocking out just one component, in our case the fatty acid transporter Cd36, is only partially able to prevent body weight gain and lipid accumulation. Our data, especially the transcriptomic data, further supports the close link between stress biology and energy metabolism, a crosstalk that is more widely recognized as stress/metabolism comorbidities emerge as complicating factors in metabolic disease and psychiatric disorders, including depression.

REFERENCES

Abumrad NA, El-Maghrabi MR, Amri EZ, Lopez E, Grimaldi PA. 1993. Cloning of a rat adipocyte membrane protein implicated in binding or transport of long-chain fatty acids that is induced during preadipocyte differentiation. Homology with human CD36. *J Biol Chem* **268**:17665–17668.

Adam EK. 2017. Diurnal Cortisol Slopes and Mental and Physical Health Outcomes:A Systematic Review and Meta-analysis. *Psychoneuroendcrinology* **Sep**:25–41. doi:110.1016/j.bbi.2017.04.008

Alkhatatbeh MJ, Enjeti AK, Acharya S, Thorne RF, Lincz LF. 2013. The origin of circulating CD36 in type 2 diabetes. *Nutr Diabetes* **3**:e59-7. doi:10.1038/nutd.2013.1

Anderson CM, Kazantzis M, Wang J, Venkatraman S, Goncalves RLS, Quinlan CL, Ng R, Jastroch M, Benjamin DI, Nie B, Herber C, Van AAN, Park MJ, Yun D, Chan K, Yu A, Vuong P, Febbraio M, Nomura DK, Napoli JL, Brand MD, Stahl A. 2015. Dependence of brown adipose tissue function on CD36-mediated coenzyme Q uptake. *Cell Rep* **10**:505–515. doi:10.1016/j.celrep.2014.12.048

Bahrami-Nejad Z, Zhao MLML, Tholen S, Hunerdosse D, Tkach KE, van Schie S, Chung M, Teruel MN. 2018. A Transcriptional Circuit Filters Oscillating Circadian Hormonal Inputs to Regulate Fat Cell Differentiation. *Cell Metab* **27**:854–868.e8. doi:10.1016/j.cmet.2018.03.012

Bartelt A, Bruns OT, Reimer R, Hohenberg H, Ittrich H, Peldschus K, Kaul MG, Tromsdorf UI, Weller H, Waurisch C, Eychmüller A, Gordts PLSM, Rinninger F, Bruegelmann K, Freund B, Nielsen P, Merkel M, Heeren J. 2011. Brown adipose tissue activity controls triglyceride clearance. *Nat Med* **17**:200–206. doi:10.1038/nm.2297

Betz MJ, Enerbäck S. 2015. Human brown adipose tissue: What we have learned so far. *Diabetes* **64**:2352–2360. doi:10.2337/db15-0146

Bowles NP, Karatsoreos IN, Li X, Vemuri VK, Wood J-A, Li Z, Tamashiro KLK, Schwartz GJ, Makriyannis AM, Kunos G, Hillard CJ, McEwen BS, Hill MN. 2015. A peripheral endocannabinoid mechanism contributes to glucocorticoid-mediated metabolic syndrome. *Proc Natl Acad Sci* **112**:285–290. doi:10.1073/pnas.1421420112

Broussard JL, Cauter E Van. 2016. Disturbances of sleep and circadian rhythms: Novel risk factors for obesity. *Curr Opin Endocrinol Diabetes Obes* **23**:353–359. doi:10.1097/MED.0000000000000276

Campbell JE, Peckett AJ, Anna MD, Hawke TJ, Riddell MC. 2011. Adipogenic and lipolytic effects of chronic glucocorticoid exposure 198–209. doi:10.1152/ajpcell.00045.2010.

Cannon B, Nedergaard J. 2004. Brown Adipose Tissue: Function and Physiological Significance. *Physiol Rev* **84**:277–359. doi:10.1152/physrev.00015.2003

Chimin P, Farias TDSM, Torres-Leal FL, Bolsoni-Lopes A, Campaña AB, Andreotti S, Lima FB. 2014. Chronic glucocorticoid treatment enhances lipogenic activity in visceral adipocytes of male Wistar rats. *Acta Physiol* **211**:409–420. doi:10.1111/apha.12226

Chusyd DE, Wang D, Huffman DM, Nagy TR. 2016. Relationships between Rodent White Adipose Fat Pads and Human White Adipose Fat Depots. *Front Nutr* **3**. doi:10.3389/fnut.2016.00010

Cypess AM, Lehman S, Williams G, Tal I, Rodman D, Goldfine AB, Kuo FC, Palmer EL, Tseng YH, Doria A, Kolodny GM, Ronald Kahn C. 2009. Identification and importance of brown adipose tissue in adult humans. *Obstet Gynecol Surv* **64**:519–520. doi:10.1097/OGX.0b013e3181ac8aa2

Dallman MF, Akana SF, Bhatnagar S, Bell ME, Strack AM. 2000. Bottomed out: Metabolic significance of the circadian trough in glucocorticoid concentrations. *Int J Obes* **24**:S40–S46.

doi:10.1038/sj.ijo.0801276

Doane LD, Mineka S, Zinbarg RE, Craske M, Griffith JW, Adam EK. 2013. Are flatter diurnal cortisol rhythms associated with major depression and anxiety disorders in late adolescence? the role of life stress and daily negative emotion. *Dev Psychopathol* **25**:629–642. doi:10.1017/S0954579413000060

Febbraio M, Abumrad NA, Hajjar DP, Sharma K, Cheng W, Pearce SFA, Silverstein RL. 1999. A null mutation in murine CD36 reveals an important role in fatty acid and lipoprotein metabolism. *J Biol Chem* **274**:19055–19062. doi:10.1074/jbc.274.27.19055

Feldmann HM, Golozoubova V, Cannon B, Nedergaard J. 2009. UCP1 Ablation Induces Obesity and Abolishes Diet-Induced Thermogenesis in Mice Exempt from Thermal Stress by Living at Thermoneutrality. *Cell Metab* **9**:203–209. doi:10.1016/j.cmet.2008.12.014

Galarraga M, Campión J, Muñoz-Barrutia A, Boqué N, Moreno H, Martínez JA, Milagro F, Ortiz-de-Solórzano C. 2012. Adiposoft: automated software for the analysis of white adipose tissue cellularity in histological sections. *J Lipid Res* **53**:2791–2796. doi:10.1194/jlr.D023788

Glatz JFC, Luiken JJFP, Bonen A. 2010. Membrane fatty acid transporters as regulators of lipid metabolism: Implications for metabolic disease. *Physiol Rev* **90**:367–417. doi:10.1152/physrev.00003.2009

Gray NE, Lam LN, Yang K, Zhou AY, Koliwad S, Wang JC. 2012. Angiopoietin-like 4 (Angptl4) protein is a physiological mediator of intracellular lipolysis in murine adipocytes. *J Biol Chem* **287**:8444–8456. doi:10.1074/jbc.M111.294124

Haemmerle G, Lass A, Zimmermann R, Gorkiewicz G, Meyer C, Rozman J, Heldmaier G, Maier R, Theussl C, Eder S, Kratky D, Wagner EF, Klingenspor M, Hoefler G, Zechner R. 2006. Defective lipolysis and altered energy metabolism in mice lacking adipose triglyceride lipase. *Science (80-)* **211**:734–738.

Hajri T, Hall AM, Jensen DR, Pietka TA, Drover VA, Tao H, Eckel R, Abumrad NA. 2007. CD36-facilitated fatty acid uptake inhibits leptin production and signaling in adipose tissue. *Diabetes* **56**:1872–1880. doi:10.2337/db06-1699

Handberg A, Norberg M, Stenlund H, Hallmans G, Attermann J, Eriksson JW. 2010. Soluble CD36 (sCD36) clusters with markers of insulin resistance, and high sCD36 is associated with increased type 2 diabetes risk. *J Clin Endocrinol Metab* **95**:1939–1946. doi:10.1210/jc.2009-2002

Harms M, Seale P. 2013. Brown and beige fat: Development, function and therapeutic potential. *Nat Med* **19**:1252–1263. doi:10.1038/nm.3361

Hauner H, Schmid P, Pfeiffer EF. 1987. Glucocorticoids and insulin promote the differentiation of human adipocyte precursor cells into fat cells. *J Clin Endocrinol Metab* **64**:832–835. doi:10.1210/jcem-64-4-832

Hodes GE, Brookshire BR, Hill-Smith TE, Teegarden SL, Berton O, Lucki I. 2012. Strain differences in the effects of chronic corticosterone exposure in the hippocampus. *Neuroscience* **222**:269–280. doi:10.1016/j.neuroscience.2012.06.017

Hoes JN, Van Der Goes MC, Van Raalte DH, Van Der Zijl NJ, Den Uyl D, Lems WF, Lafeber FPGJ, Jacobs JWG, Welsing PMJ, Diamant M, Bijlsma JWJ. 2011. Glucose tolerance, insulin sensitivity and β-cell function in patients with rheumatoid arthritis treated with or without low-to-medium dose glucocorticoids. *Ann Rheum Dis* **70**:1887–1894. doi:10.1136/ard.2011.151464

Karatsoreos IN, Bhagat SM, Bowles NP, Weil ZM, Pfaff DW, McEwen BS. 2010. Endocrine and physiological changes in response to chronic corticosterone: A potential model of the metabolic syndrome in mouse. *Endocrinology* **151**:2117–2127. doi:10.1210/en.2009-1436

Ketzer LA, Mousovich-Neto F, de Melo Reis RA, Atella GC, Carvalho DP, Costa ACR, Corrêa da Costa VM, Matos MS, Miranda-Alves L. 2019. Brown adipose tissue remodeling induced by corticosterone in Wistar male rats. *Exp Physiol* 1–15. doi:10.1113/ep087332

Koliwad SK, Kuo T, Shipp LE, Gray NE, Backhed F, So AYL, Farese R V., Wang JC. 2009. Angiopoietin-like 4 (ANGPTL4, fasting-induced adipose factor) is a direct glucocorticoid receptor target and participates in glucocorticoid-regulated triglyceride metabolism. *J Biol Chem* **284**:25593–25601. doi:10.1074/jbc.M109.025452

Koonen DPY, Sung MMY, Kao CKC, Dolinsky VW, Koves TR, Ilkayeva O, Jacobs RL, Vance DE, Light PE, Muoio DM, Febbraio M, Dyck JRB. 2010. Alterations in skeletal muscle fatty acid handling predisposes middle-aged mice to diet-induced insulin resistance. *Diabetes* **59**:1366–1375. doi:10.2337/db09-1142

Kumari M, Badrick E, Chandola T, Adam EK, Stafford M, Marmot MG, Kirschbaum C, Kivimaki M. 2009. Cortisol secretion and fatigue: Associations in a community based cohort. *Psychoneuroendocrinology* **34**:1476–1485. doi:10.1016/j.psyneuen.2009.05.001

Kusminski CM, Bickel PE, Scherer PE. 2016. Targeting adipose tissue in the treatment of obesity-associated diabetes. *Nat Rev Drug Discov* **15**:639–660. doi:10.1038/nrd.2016.75

Lee M-J, Pramyothin P, Karastergiou K, Fried SK. 2014. Deconstructing the roles of glucocorticoids in adipose tissue biology and the development of central obesity. *Biochim Biophys Acta* **1842**:473–481. doi:10.1016/j.bbadis.2013.05.029

Lee RA, Harris CA, Wang J-C. 2018. Glucocorticoid Receptor and Adipocyte Biology. *Nucl Recept Res* **5**:1–21. doi:10.32527/2018/101373

Lekkas D, Paschos GK. 2019. Autonomic Neuroscience : Basic and Clinical The circadian clock control of adipose tissue physiology and metabolism. *Auton Neurosci Basic Clin* **219**:66–70. doi:10.1016/j.autneu.2019.05.001

Lightman S, Terry JR. 2014. The importance of dynamic signalling for endocrine regulation and drug development: Relevance for glucocorticoid hormones. *Lancet Diabetes Endocrinol* **2**:593–599. doi:10.1016/S2213-8587(13)70182-7

Liu J, Kong X, Wang L, Qi H, Di W, Zhang X, Wu L, Chen X, Yu J, Zha J, Lv S, Zhang A, Cheng P, Hu M, Li Y, Bi J, Li Y, Hu F, Zhong Y, Xu Y, Ding G. 2012. Essential roles of 11β-HSD1 in regulating brown adipocyte function. *J Mol Endocrinol* **50**:103–113. doi:10.1530/JME-12-0099

Luijten IHN, Brooks K, Boulet N, Shabalina IG, Jaiprakash A, Carlsson B, Fischer AW, Cannon B, Nedergaard J. 2019a. Glucocorticoid-Induced Obesity Develops Independently of UCP1. *Cell Rep* **27**:1686–1698.e5. doi:10.1016/j.celrep.2019.04.041

Luijten IHN, Cannon B, Nedergaard J. 2019b. Glucocorticoids and Brown Adipose Tissue: Do glucocorticoids really inhibit thermogenesis? *Mol Aspects Med* **68**:42–59. doi:10.1016/j.mam.2019.07.002

Matthews K, Schwartz J, Cohen S, Seeman T. 2006. Diurnal cortisol decline is related to coronary calcification: CARDIA study. *Psychosom Med* **68**:657–661. doi:10.1097/01.psy.0000244071.42939.0e

Miller GE, Chen E, Zhou ES. 2007. If it goes up, must it come down? Chronic stress and the hypothalamic-pituitary-adrenocortical axis in humans. *Psychol Bull* **133**:25–45. doi:10.1037/0033-2909.133.1.25

Nagy L, Tontonoz P, Alvarez JGA, Chen H, Evans RM. 1998. Oxidized LDL regulates macrophage gene expression through ligand activation of PPARγ. *Cell* **93**:229–240. doi:10.1016/S0092-8674(00)81574-3

Paschos GK, Ibrahim S, Song W, Kunieda T, Reyes TM, Bradfield CA, Vaughan CH, Eiden M, Masoodi M, Griffin JL, Wang F, Lawson JA, Garret A. 2013. Obesity in mice with adipocyte-specific deletion of clock component Arntl. *Nat Med* **18**:1768–1777. doi:10.1038/nm.2979.Obesity

Peckett AJ, Wright DC, Riddell MC. 2011. The effects of glucocorticoids on adipose tissue lipid metabolism. *Metabolism* **60**:1500–1510. doi:10.1016/j.metabol.2011.06.012

Pepino MY, Kuda O, Samovski D, Abumrad NA. 2014. Structure-Function of CD36 and Importance of Fatty Acid Signal Transduction in Fat Metabolism. *Annu Rev Nutr* **34**:281–303. doi:10.1146/annurev-nutr-071812-161220

Ramage LE, Akyol M, Fletcher AM, Forsythe J, Nixon M, Carter RN, van Beek EJR, Morton NM, Walker BR, Stimson RH. 2016. Glucocorticoids Acutely Increase Brown Adipose Tissue Activity in Humans, Revealing Species-Specific Differences in UCP-1 Regulation. *Cell Metab* **24**:130–141. doi:10.1016/j.cmet.2016.06.011

Rosen ED, MacDougald O a. 2006. Adipocyte differentiation from the inside out. *Nat Rev Mol Cell Biol* **7**:885–96. doi:10.1038/nrm2066

Saito M. 2013. Brown adipose tissue as a regulator of energy expenditure and body fat in humans. *Diabetes Metab J* **37**:22–29. doi:10.4093/dmj.2013.37.1.22

Saito M, Okamatsu-Ogura Y, Matsushita M, Watanabe K, Yoneshiro T, Nio-Kobayashi J, Iwanaga T, Miyagawa M, Kameya T, Nakada K, Kawai Y, Tsujisaki M. 2009. High incidence of metabolically active brown adipose tissue in healthy adult humans: Effects of cold exposure and adiposity. *Diabetes* **58**:1526–1531. doi:10.2337/db09-0530

Samovski D, Dhule P, Pietka T, Jacome-Sosa M, Penrose E, Son NH, Flynn CR, Shoghi KI, Hyrc KL, Goldberg IJ, Gamazon ER, Abumrad NA. 2018. Regulation of insulin receptor pathway and glucose metabolism by CD36 signaling. *Diabetes* **67**:1272–1284. doi:10.2337/db17-1226

Schäcke H, Döcke WD, Asadullah K. 2002. Mechanisms involved in the side effects of glucocorticoids. *Pharmacol Ther* **96**:23–43. doi:10.1016/S0163-7258(02)00297-8

Sephton SE, Lush E, Dedert EA, Floyd AR, Rebholz WN, Dhabhar FS, Spiegel D, Salmon P. 2013. Diurnal cortisol rhythm as a predictor of lung cancer survival. *Brain Behav Immun* **30**. doi:10.1016/j.bbi.2012.07.019

Shen Y, Roh HC, Kumari M, Rosen ED. 2017. Adipocyte glucocorticoid receptor is important in lipolysis and insulin resistance due to exogenous steroids, but not insulin resistance caused by high fat feeding. *Mol Metab* **6**:1150–1160. doi:10.1016/j.molmet.2017.06.013

Shostak A, Meyer-Kovac J, Oster H. 2013. Circadian regulation of lipid mobilization in white adipose tissues. *Diabetes* **62**:2195–2203. doi:10.2337/db12-1449

Sidossis L, Kajimura S. 2015. Brown and beige fat in humans: Thermogenic adipocytes that control energy and glucose homeostasis. *J Clin Invest* **125**:478–486. doi:10.1172/JCI78362

Strack a M, Bradbury MJ, Dallman MF. 1995. Corticosterone decreases nonshivering thermogenesis and increases lipid storage in brown adipose tissue. *Am J Physiol* **268**:R183–R191. doi:10.1152/ajpregu.1995.268.1.R183

Tontonoz P, Nagy L, Alvarez JGA, Thomazy VA, Evans RM. 1998. PPARγ promotes monocyte/macrophage differentiation and uptake of oxidized LDL. *Cell* **93**:241–252. doi:10.1016/S0092-8674(00)81575-5

Van Den Beukel JC, Grefhorst A, Quarta C, Steenbergen J, Mastroberardino PG, Lombés M, Delhanty PJ, Mazza R, Pagotto U, Van Der Lely AJ, Themmen APN. 2014. Direct activating effects of adrenocorticotropic hormone (ACTH) on brown adipose tissue are attenuated by corticosterone. *FASEB J* **28**:4857–4867. doi:10.1096/fj.14-254839

Van Marken Lichtenbelt WD, Vanhommerig JW, Smulders NM, Drossaerts JMAFL, Kemerink GJ, Bouvy ND, Schrauwen P, Teule GJJ. 2009. Cold-activated brown adipose tissue in healthy men. *N Engl J Med* **360**:1500–1508. doi:10.1056/NEJMoa0808718

Vroegrijk IOCM, Van Klinken JB, Van Diepen JA, Van Den Berg SAA, Febbraio M, Steinbusch LKM, Glatz JFC, Havekes LM, Voshol PJ, Rensen PCN, Van Dijk KW, Van Harmelen V. 2013. CD36 is important for adipocyte recruitment and affects lipolysis. *Obesity* **21**:2037–2045. doi:10.1002/oby.20354

Weitzman ED, Fukushima D, Nogeire C, Roffwarg H, Gallagher TF, Hellman L. 1971. Twenty-four hour pattern of the episodic secretion of cortisol in normal subjects. *J Clin Endocrinol Metab* **33**:14–22. doi:10.1210/jcem-33-1-14

Yang J, Park KW, Cho S. 2018. Inhibition of the CD36 receptor reduces visceral fat accumulation and improves insulin resistance in obese mice carrying the BDNF-Val66Met variant. *J Biol Chem* **293**:13338–13348. doi:10.1074/jbc.RA118.002405

Yu CY, Mayba O, Lee J V., Tran J, Harris C, Speed TP, Wang JC. 2010. Genome-wide analysis of glucocorticoid receptor binding regions in adipocytes reveal gene network involved in triglyceride homeostasis. *PLoS One* **5**. doi:10.1371/journal.pone.0015188

AUTHOR CONTRIBUTIONS

S.T. and M.N.T. conceived the project. S.T. performed and analyzed all experiments with assistance of A.R., E.B.M., and W.Y. K.K. analyzed transcriptomic data. S.T. and M.N.T wrote the paper with input from all authors.

ACKNOWLEDGEMENTS

This work was supported by National Institutes of Health RO1-DK101743, RO1-DK106241, P50-GM107615, and Stanford BioX Seed Grant funding (to M.N.T.). Furthermore we acknowledge the funding from the Deutsche Forschungsgemeinschaft (DFG) TH 2156/1-1 (to S.T). We thank all members of the Teruel Lab for discussions and critical reading of the manuscript. We also thank the Stanford Animal Histology Services (AHS) for paraffin embedding of fat tissue and performing H&E staining.

FIGURE LEGENDS

Fig. 1: Time course analysis of lipid accumulation in WAT induced by flattening of circadian corticosterone oscillations. (A) Time course of average corticosterone levels in mice implanted with corticosterone pellets compared to mice implanted with sham pellets 7 days after pellet implantation. n = 3 for sham pellet; n = 4 for corticosterone pellet, mean ± SEM. **(B)** Time course showing body weight gain of mice implanted with corticosterone pellets compared to mice implanted with sham pellets. n = 11, mean ± SEM. Unpaired t test (sham pellet versus cort pellet), *$p < 0.05$, **$p < 0.01$, ***$p < 0.001$, ****$p < 0.0001$. **(C)** Average daily food intake of each mouse per cage (n = 8). Up to 5 mice were housed in each cage. Food intake was monitored for 14 days, mean ± SD. Unpaired t test, ns = not significant. **(D)** sWAT after pellet implantation for 21 days. **(E)** Weight of sWAT at different time points after pellet implantation, n = 5-9, mean ± SD. Unpaired t test, **$p < 0.01$, ****$p < 0.0001$. **(F)** vWAT after pellet implantation for 21 days. **(G)** Weight of vWAT at different time points after pellet implantation, n = 5-9, mean ± SD. Unpaired t test, *$p < 0.05$, ****$p < 0.0001$. **(H)** Time course of sWAT after pellet implantation. WAT was stained with hematoxylin and eosin at 3, 7, 14, and 21 days after pellet implantation. One representative staining is shown (n = 3). Scale bars 50μm. **(I)** Frequency distribution of mean adipocyte area in sWAT as analyzed using Adiposoft (mean + SEM; n=3 mice per treatment, 25 images per mouse (20x)). **(J)** Time course of vWAT after pellet implantation. WAT was stained with hematoxylin and eosin at 3, 7, 14, and 21 days after pellet implantation. One representative staining is shown (n = 3). Scale bars 50μm. **(K)** Frequency distribution of mean adipocyte area in vWAT as analyzed using Adiposoft (mean + SEM; n=3-4 mice per treatment, 25 images per mouse (20x)).

Fig. 2: Increasing the peak amplitude of corticosterone in the evening phase does not affect body weight gain or lipid accumulation in WAT. (A) Time course of average corticosterone levels in mice injected with corticosterone compared to mice injected with solvent control 7 days after start of injections. n = 3-4, mean ± SEM. **(B)** Time course showing body weight gain of mice implanted with corticosterone pellets compared to mice implanted with sham pellets. n = 9, mean ± SEM. **(C)** Average daily food intake of each mouse per cage (n = 7). Up to 5 mice were housed in each cage. Food intake was monitored for 14 days, mean ± SD. Unpaired t test, **$p < 0.01$, ns = not significant. **(D)** sWAT of sham and corticosterone injected mice 21 days after start of treatment. **(E)** Weight of sWAT at different time points after start of daily injections, n = 3-8, mean ± SD. **(F)** Time course of sWAT after start of injections. WAT was stained with hematoxylin and eosin at 3, 7, 14, and 21 days after start of treatment. One representative staining is shown (n = 3). Scale bars 50μm. **(G)** vWAT of sham and corticosterone injected mice 21 days after start of treatment. **(H)** Weight of vWAT at different time points after start of daily injections, n = 3-8, mean ± SD. **(I)** Time course of vWAT after start of injections. WAT was stained with hematoxylin and eosin at 3, 7, 14, and 21 days after start of treatment. One representative staining is shown (n = 3). Scale bars 50μm.

Fig. 3: Flattening of daily corticosterone oscillations in mice results in lipid accumulation in BAT. (A) Interscapular BAT of sham and corticosterone pellet implanted mice 14 days after start of treatment. **(B)** Weight of interscapular BAT at different time points after pellet implantation, n = 5-9, mean ± SD. Unpaired t test, **$p < 0.01$, ****$p < 0.0001$. **(C)** Time course of BAT after pellet implantation. BAT was stained with hematoxylin and eosin at 3, 7, 14, and 21 days after pellet implantation. One representative staining is shown (n = 3-7). Scale bars 50μm. **(D)** Frequency distribution of mean adipocyte area in BAT as analyzed using Adiposoft (mean + SEM; for day 3, 7, 14 n = 3; for day 21 n = 5 mice per treatment, 25 images per mouse (20x)). **(E)** BAT of sham and corticosterone injected mice 14 days after start of treatment. **(F)** Weight of BAT at different time points after start of daily

injections, n = 3-8, mean ± SD. **(G)** Time course of BAT after start of injection. BAT was stained with hematoxylin and eosin at 3, 7, 14, and 21 days after start of injection. One representative staining is shown (n = 3-7). Scale bars 50μm

Fig. 4: Flattening of corticosterone oscillations does not elevate circulating triglycerides in blood or result in fat deposition in the liver. (A) H&E staining of livers 21 days after pellet implantation / start of injection. One representative staining is shown (n = 4). **(B)** Weight of livers at different time points after pellet implantation, n = 4-5, mean ± SD. **(C)** Weight of livers at different time points after start of daily injections, n = 3-4, mean ± SD. **(D-I)** Time courses of changes in FFA, glycerol, and triglycerides measured in blood serum over 14 days. n = 4-5 for pellet implanted mice, n = 3-4 for injected mice, mean ± SEM, unpaired t test, *p < 0.05, ns = not significant.

Fig. 5: Flattening of corticosterone oscillations causes hyperinsulinemia. (A) Glucose tolerance test (GTT) of sham and corticosterone pellet implanted mice after 21 days of treatment; mean ± SEM; n = 5; unpaired t test, *p < 0.05, ***p < 0.001, ****p < 0.0001. **(B)** Insulin tolerance test (ITT) of sham and corticosterone pellet implanted mice after 17 days of treatment; mean ± SEM; n = 5 for sham pellet; n = 6 for corticosterone pellet; unpaired t test, *p < 0.05, **p < 0.01. **(C)** Glucose tolerance test (GTT) of sham and corticosterone injected mice after 21 days of treatment; mean ± SEM; n = 6. **(D)** Insulin tolerance test (ITT) of sham and corticosterone injected mice after 17 days of treatment; mean ± SEM; n = 5 for sham injection; n = 6 for corticosterone injection. **(E)** Time course of insulin levels in blood plasma in sham and corticosterone pellet implanted mice (not fasted); mean +/- SEM; n = 6; unpaired t test, *p < 0.05, **p < 0.01, ****p < 0.0001. **(F)** Blood glucose levels in sham and corticosterone pellet implanted mice (not fasted) 14 days after pellet implantation; mean +/- SEM; n = 9; unpaired t test, **p < 0.01.

Fig. 6: Transcriptomic analysis of vWAT reveals expression alterations due to flattening of corticosterone oscillations. (A) Hierarchical clustering of vWAT samples of corticosterone and sham pellet implanted mice 0, 3, 7, and 14 days after pellet implantation. **(B)** GO terms in the category Biological Process altered in corticosterone pellet implanted mice categorized based on common topics. **(C)** Selected GO terms in the category Biological Process altered in corticosterone pellet implanted mice. Differently expressed genes were rated according to their p-value (< 0.05) and their fold change (cutoff 1.5). Number of genes for each GO term is presented in brackets. **(D)** Differently expressed genes (FC cutoff 1.5) comparing vWAT of sham and corticosterone pellet implanted mice.

Fig. 7: Transcriptomic analysis of BAT reveals expression alterations due to flattening of corticosterone oscillations. (A) Hierarchical clustering of BAT samples of corticosterone and sham pellet implanted mice 0, 3, 7, and 14 days after pellet implantation. **(B)** GO terms in the category Biological Process alterd in BAT of cort pellet implanted mice categorized based on common topics. **(C)** Selected GO terms in the category Biological Process altered in corticosterone pellet implanted mice. Differently expressed genes were rated according to their p-value (< 0.05) and their fold change (cutoff 1.5). Number of genes for each GO term is presented in brackets. **(D)** Heatmap of differently expressed genes altered either in BAT or vWAT (FC cutoff 1.5) comparing sham and corticosterone pellet implanted mice. **(E)** mRNA expression for Ucp-1 and Pgc1a measured by qPCR in BAT of sham and corticosterone pellet implanted mice 3, 7, and 14 days after implantation. Gene expression data was normalized to the expression of Tbp and is presented as mean ± SEM (n = 3-4). Unpaired t test, *p < 0.05, **p < 0.01, ***p < 0.001, ns = not significant. Control group are mice at start of experiment (day 0).

Fig. 8: Cd36ko partially protects against fat gain due to flattening of corticosterone oscillations. **(A)** mRNA expression for Cd36 measured by qPCR in vWAT and BAT of sham and corticosterone pellet implanted mice 3 and 14 days after implantation. Gene expression data was normalized to the expression of Tbp and is presented as mean ± SEM (n = 3-4). Unpaired t test, *p < 0.05, **p < 0.01, ***p < 0.001, ns = not significant. Control group are mice at start of experiment (day 0). **(B)** Time course showing body weight gain of wild type and Cd36ko mice implanted with corticosterone pellets compared to mice implanted with sham pellets. n = 10-12, mean ± SEM. Unpaired t test (red asterisk: WT + sham pellet versus Cd36ko + sham pellet; blue asterisk: WT + corticosterone pellet versus Cd36ko + corticosterone pellet; black asterisk: sham versus corticosterone pellet), *p < 0.05, **p < 0.01, ***p < 0.001, ****p < 0.0001. **(C)** Weight of epididymal (visceral) fat depots 21 days after pellet implantation, n = 5-12, mean ± SD. Unpaired t test, *p < 0.05, ****p < 0.0001. **(D)** H&E staining of vWAT 21 days after pellet implantation. One representative staining is shown (n = 3-5). Scale bars 50μm. **(E)** Frequency distribution of mean adipocyte area in vWAT as analyzed using Adiposoft (mean + SEM; n=3-5, 25 images per mouse (20x)). **(F)** Weight of inguinal (subcutaneous) fat depots 21 days after pellet implantation, n = 5-12, mean ± SD. Unpaired t test, ****p < 0.0001. **(G)** H&E staining of sWAT 21 days after pellet implantation. One representative staining is shown (n = 4-5). Scale bars 50μm. **(H)** Frequency distribution of mean adipocyte area in sWAT as analyzed using Adiposoft (mean + SEM; n=4-5, 25 images per mouse (20x)). **(I)** Weight of BAT 21 days after pellet implantation, n = 5-12, mean ± SD. Unpaired t test, *p < 0.05, ***p < 0.001, ****p < 0.0001. **(J)** H&E staining of BAT 21 days after pellet implantation. One representative staining is shown (n = 4-5). Scale bars 50μm. **(K)** Frequency distribution of mean adipocyte area in BAT as analyzed using Adiposoft (mean + SEM; n=4-5, 25 images per mouse (20x)).

Sup. Fig. 1: Flattening of corticosterone oscillations does not result in significant gene expression alterations of genes involved in lipid metabolism. (A-J) Gene expression of different genes measured by qPCR in liver after flattening corticosterone levels for 14 days. Gene expression data was normalized to the expression of Tbp and is presented as mean ± SEM (n = 3-4). Unpaired t test, *p < 0.05, **p < 0.01, ns = not significant. Control group are mice at beginning of experiment (day 0).

Sup. Fig. 2: Transcriptomic analysis of vWAT and BAT reveals little expression alterations due to injection of corticosterone increasing the corticosterone amplitude in the waking phase. Hierarchical clustering of vWAT **(A)** and BAT **(B)** samples of corticosterone and sham pellet injected mice 0, 3, 7, and 14 days after first injection.

Sup. Fig. 3: Flattening of corticosterone oscillations in mice does not affect thermogenesis. Acute cold exposure experiment of sham and corticosterone pellet implanted mice 21 days after pellet implantation. Mean +/- SEM; n = 8.

Sup. Fig. 4: Cd36ko mice are not protected against hyperinsulinemia caused by flattening of corticosterone. (A) Insulin levels in blood plasma in sham and corticosterone pellet implanted Cd36ko and wild-type mice (not fasted) 14 days after pellet implantation; mean +/- SEM; n = 5-7; unpaired t test, *p < 0.05, **p < 0.01. **(B)** Blood glucose levels in sham and corticosterone pellet implanted

Cd36ko and wild-type mice (not fasted) 14 days after pellet implantation; mean +/- SEM; n = 6-9; unpaired t test, **$p < 0.01$.

Sup. Table 1: Summary of mouse experiments. All data was acquired after a treatment period of 21 days, except data for blood glucose (not fasted), FFA, glycerol, and triglyceride levels, which were determined 14 days after beginning of treatment. Values are presented as mean +/- SEM; n.d. = no data

Sup. Table 2: Gene expression levels comparing vWAT of corticosterone and sham pellet implanted mice. Genes are considered differently expressed with a fold change of 1.5 and p value < 0.05.

Sup. Table 3: Gene ontology (GO) analysis of RNAseq data comparing vWAT of corticosterone and sham pellet implanted mice. Genes were considered differently expressed with a fold change of 1.5 and p value < 0.05.

Sup. Table 4: Gene expression levels comparing BAT of corticosterone and sham pellet implanted mice. Genes are considered differently expressed with a fold change of 1.5 and p value < 0.05.

Sup. Table 5: Gene ontology (GO) analysis of RNAseq data comparing BAT of corticosterone and sham pellet implanted mice. Genes were considered differently expressed with a fold change of 1.5 and p value < 0.05.

METHODS

Mice

Mice were housed in small groups of five or fewer on a 12h light/dark cycle (lights on at 7:00 hours) with food and water access ad libitum in the animal facility at Stanford University. All mice were maintained on a normal chow diet and only male mice were used for experiments. All animal care and experimentation was conducted in accordance with current NIH and Stanford University Institutional Animal Care and Use Committee guidelines. Seven-week-old C57BL/6J male mice were purchased from Jackson Laboratory (cat. 000664) and housed in the animal facility for 7 days prior the start of experiments. Cd36ko mice were published before (Febbraio et al., 1999). Cd36ko breeding pairs were purchased from Jackson Laboratory (cat. 019006). For the experiments 8 week old male mice were used. All mice were dissected between 13:00 and 18:00 alternating corticosterone treated and control mice.

Corticosterone administration in mice

To flatten circadian glucocorticoid oscillations mice were implanted subcutaneously with corticosterone releasing pellets (5mg, 21 day release; Innovative Research of America, Sarasota, FL, USA). Placebo pellets were implanted as control. For pellet implantation mice were anesthetized via inhalation of isoflurane, when anesthetized an incision equal in diameter to that of the pellet was made on the lateral side of the neck and the pellet inserted using a trochar. Mice weighed an average of 24.1 ± 1.2 g, which results in a daily dose of 9 mg/kg/day.

For injections, corticosterone complexed with 2-hydroxypropyl-β-cyclodextrin (C174, Sigma) was dissolved in PBS and injected subcutaneously once daily at 17:00 for up to 21 days with the same corticosterone dose (9 mg/kg/day) as released by the corticosterone pellets per day.

Measurement of corticosterone in blood serum

Blood was taken at multiple time points over a 15 h time period. At the first time point blood was taken by nicking the tail vain. Blood samples collected on following time points were taken by removal of the crust formed after first blood withdrawal. The blood was allowed to clot by leaving it undisturbed at room temperature for 45 minutes. The clot was removed by centrifuging at 2000 x g for 15 minutes. The corticosterone concentration in blood serum was determined using the Enzyme Immunoassay kit (K014-H1, Arbor Assays, Michigan, USA) following the manufacturer's instructions.

Glucose Tolerance Test

Before the procedure mice were fasted for 16h in clean cages with no food or feces in the bedding. At 9am blood glucose levels were measured with a glucometer (Diathrive, South Salt Lake, Utah, USA) by obtaining a drop of blood from the tail. Subsequently, mice received 2 g of glucose (Sigma G8270) / kg of body weight by intraperitoneal injection. Blood glucose levels were measured again after 15, 30, 60, and 120 min after injection.

To measure insulin levels, 20 μl of blood were collected from the tail before glucose injection and on every following time point and mixed with heparin. The blood plasma was prepared by centrifugation at 2000 x g for 15 minutes. The insulin concentration in blood plasma was determined using the Ultra Sensitive Mouse Insulin ELISA Kit (Cat. 90080, Crystal Chem, Illinois, USA) following the manufacturer's instructions.

Insulin Tolerance Test

Before the procedure mice were fasted for 6h in clean cages with no food or feces in the bedding starting at 9am. Blood glucose levels were measured with a glucometer (Diathrive, South Salt Lake, Utah, USA) by obtaining a drop of blood from the tail. Subsequently, mice were injected with 0.75 units/kg body weight of human insulin (Sigma I9278) by intraperitoneal injection. Blood glucose levels were measured again after 15, 30, 45, 60, and 120 min after injection.

To measure insulin levels 20 μl of blood were collected from the tail before glucose injection and on every following time point and mixed with heparin. The blood plasma was prepared by centrifugation at 2000 x g for 15 minutes. The insulin concentration in blood plasma was determined using the Ultra Sensitive Mouse Insulin ELISA Kit (Cat. 90080, Crystal Chem, Illinois, USA) following the manufacturer's instructions.

Histology

For histological examination interscapular brown adipose tissue (BAT), inguinal white adipose tissue (sWAT), and epididymal white adipose tissue (vWAT) were fixed in 4% formalin for 24h directly after dissection. Tissues were rinsed and stored in 95% until embedding in paraffin. Paraffin blocks were sectioned (10μm) and sections mounted on glass slides and stained with hematoxylin and eosin (H & E). Images were taken at 20x magnification and the adipocyte area was calculated using the Fiji software plug-in Adiposoft (Galarraga et al., 2012).

Acute cold exposure

Mice were housed individually with minimal bedding and exposed to 6°C for 6 hours with free access to water. Core body temperatures were measured with a rectal probe thermometer (Type J/K/T Thermocouple meter, Digisense, Kentscientific, USA; with rectal probe for mice RET-3, Physitemp Instruments, USA) before and indicated intervals during cold exposure. After 6 hours of cold exposure mice were sacrificed and tissues were harvested.

Reverse transcription quantitative polymerase chain reaction

Total RNA was extracted from fat tissues using the RNeasy Lipid Tissue Mini Kit (Qiagen, Hilden, Germany) and from liver using the RNeasy Mini Kit (Qiagen, Hilden, Germany). Equal amounts of RNA were reverse-transcribed to cDNA using the iScript cDNA Synthesis system (Bio-Rad, Hercules, CA, USA). Relative transcript amounts were measured by qPCR using PowerUp SYBR Green Master

Mix (Appliedbiosystems, Vilnius, Lithuania). All expression data were normalized to TATA-binding protein expression.

RNAseq

RNA was extracted from BAT or vWAT using the RNeasy Lipid Tissue Mini Kit (Qiagen, Hilden, Germany). For each condition (sham pellet, corticosterone pellet, sham injection, corticosterone injection) RNA was extracted from 4 mice per time point (3, 7, 14 days). RNA was also isolated from 4 mice before start of treatment (day 0). RNA quality of all samples was evaluated by Bioanalyzer 2100 High Sensitivity RNA Analysis chips (Agilent, Cat. 5067-1513) which displayed intact RNA integrity. mRNA samples were concentrated to ≤ 5 μl by MinElute column (QIAGEN, Cat. 74204). For generation of RNA-seq libraries, polyadenylated mRNA was isolated from 300 ng of total RNA by incubation with oligo-DT attached magnetic beads and followed by strand-specific library preparation using the TruSeq Stranded mRNA Library Preparation kit (Ilumina, Cat. 20020595). Briefly, isolated polyadenylated mRNA was fragmented using divalent cations under elevated temperature and 1st and 2nd strands DNA were synthesized using SuperScript II Reverse Transcriptase (provided with Ilumina kit). A-tailing and adapter ligation was performed according to the manufacturer's protocol; the resulting dsDNA was enriched in a PCR reaction based on predetermined CT values and cleaned using AMPure XP beads (provided with Ilumina kit). Concentrations of enriched dsDNA fragments with specific adapters were determined and base pair average size as well as library integrity were analyzed using the Bioanalyzer DNA High Sensitivity chips (Agilent, Cat. 5067-4626). Samples were pooled and sequenced on the Illumina NextSeq 500/550 High Output platform (Illumina, FC-404-2002) up to 18 samples per lane with 1% PhiX spike as a control.

The read quality of the raw FASTQ files was checked with FastQC (Andrews and Babraham Bioinformatics, 2010) (v0.11.7). Next, reads were pseudo-aligned to the mouse reference transcriptome (Mus_musculus.GRCm38.cdna) using Kallisto(Bray et al., 2016) (v0.44.0) with the quantification algorithm enabled, the number of bootstraps set to 100, and run in paired-end mode.

The Kallisto output files were read into R using Sleuth, and the transcripts per million (TPM), a measurement of the proportion of transcripts in the RNA pool, was used for downstream differential expression analysis (Pimentel et al., 2017).

Measuring concentrations of FFA, glycerol, and triglycerides

FFA contents in blood serum were determined the Free Fatty Acid Quantitation Kit (Sigma, MAK044) following the manufacturers' protocols. Glycerol and triglyceride concentrations in blood serum were measured using the Triglyceride Determination Kit (Sigma, TR0100) following the manufacturer's instructions.

Statistics

All data are represented as mean ± SD or mean ± SEM and analyzed by Students t test using GraphPad Prism software. n indicates the number of animals per group or number of independent experiments. Results were considered significant if $p < 0.05$.

Fig. 1

Tholen et al.

A

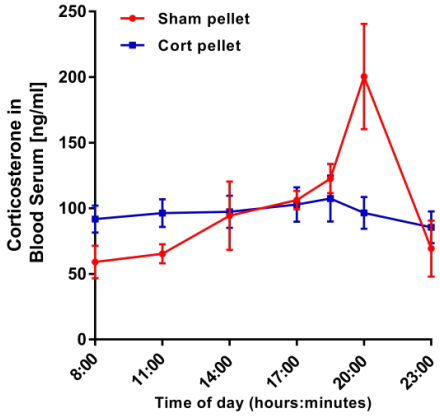

B

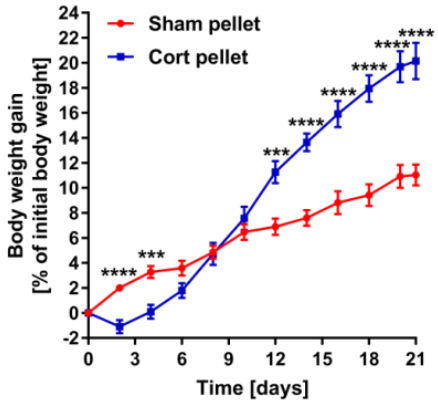

C

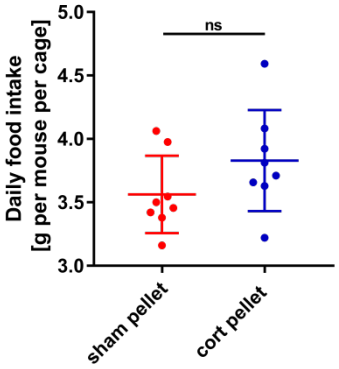

D

E

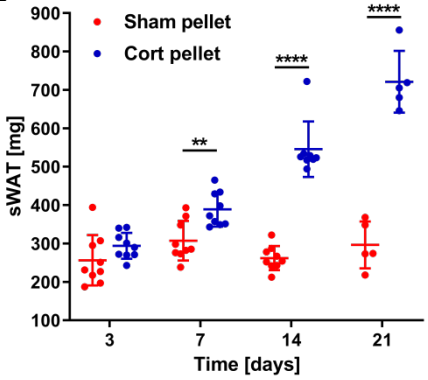

F

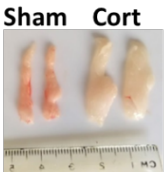

G

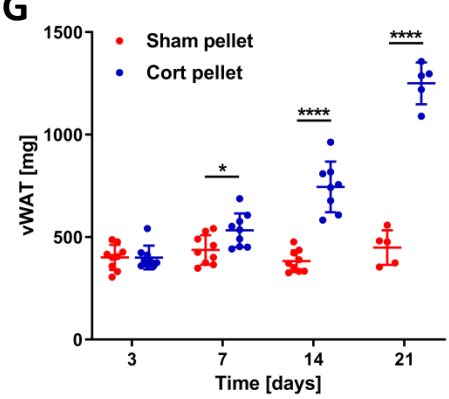

H

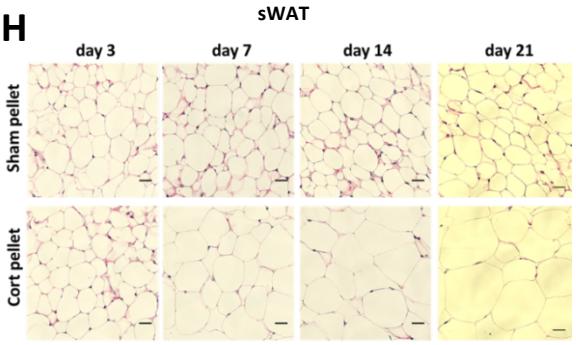

I

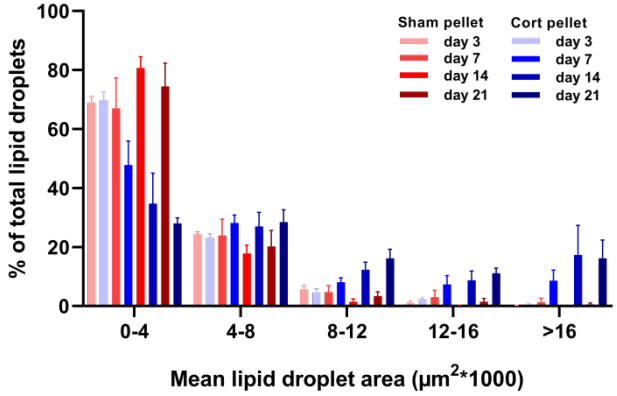

J

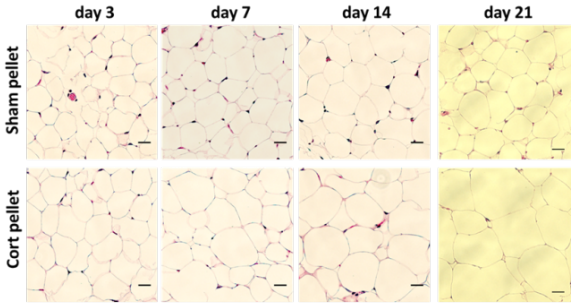

K

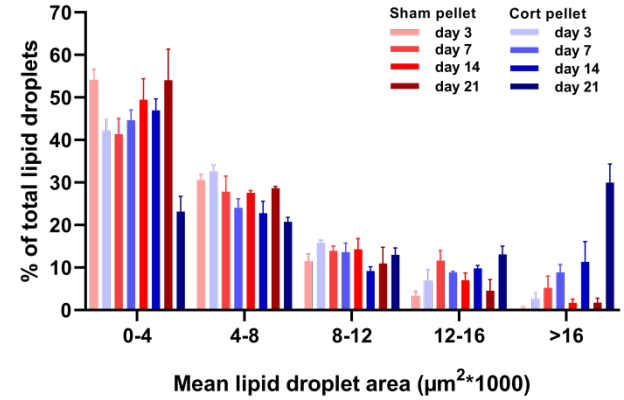

Fig. 2

Tholen et al.

A

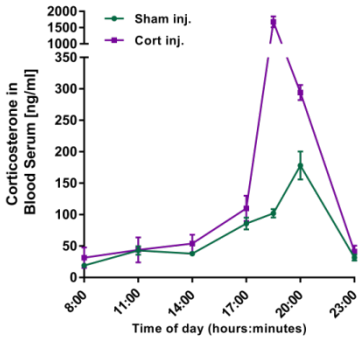

B

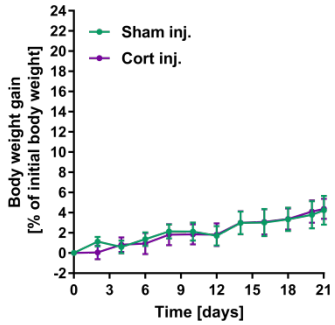

C

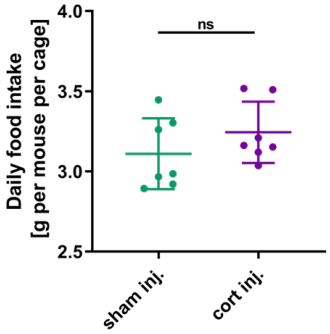

D

E

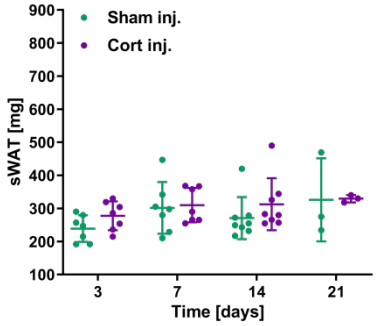

F

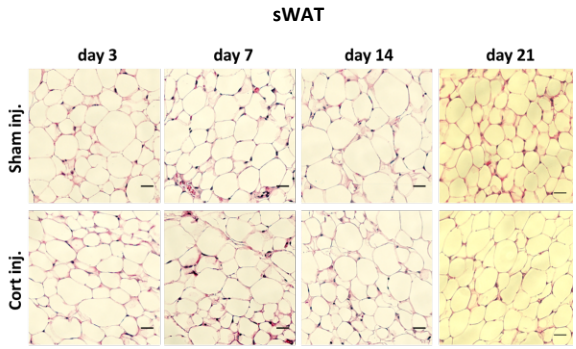

G

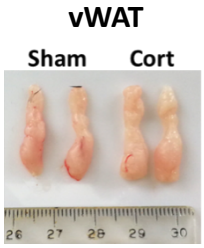

H

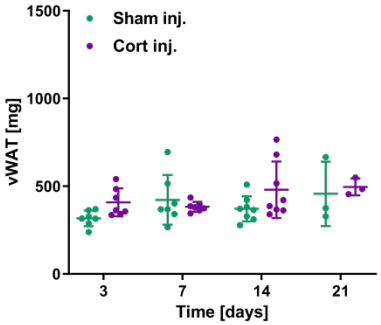

I

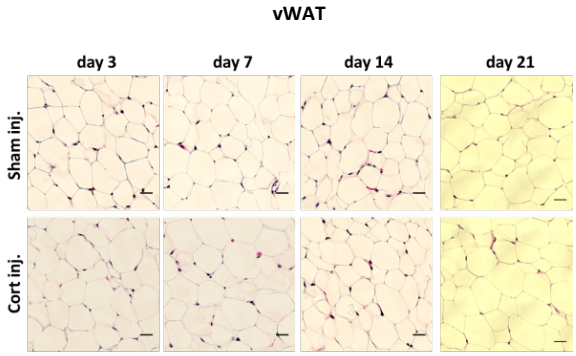

Fig. 3

Tholen et al.

A

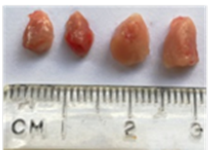

B

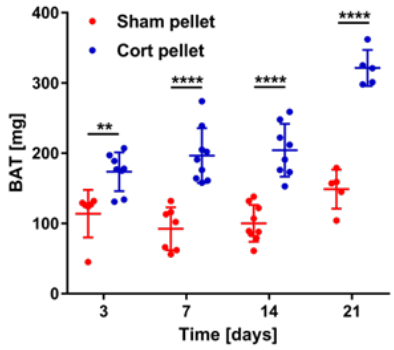

C

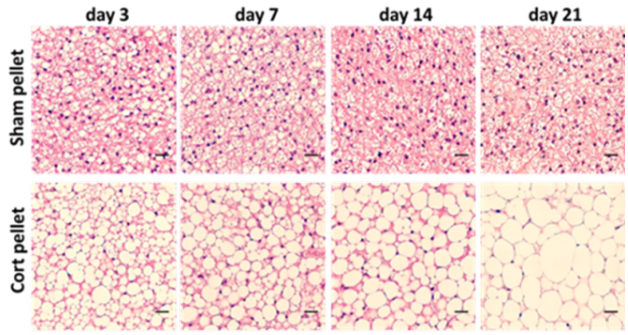

D

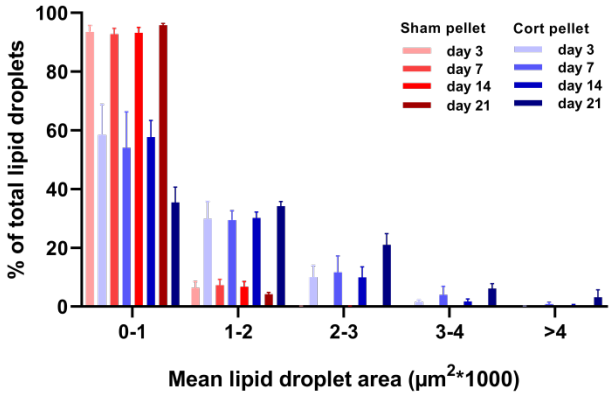

E

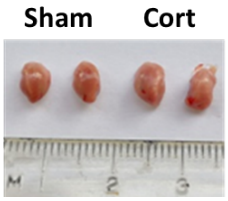

F

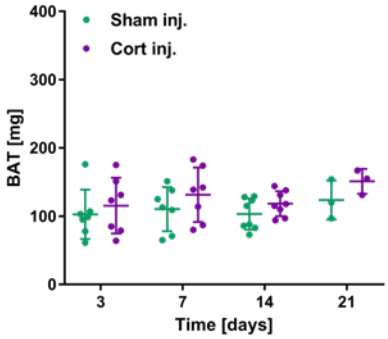

G

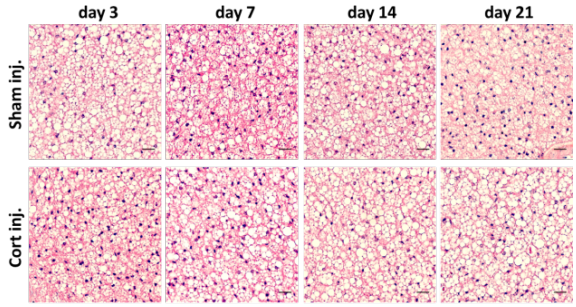

Fig. 4

Tholen et al.

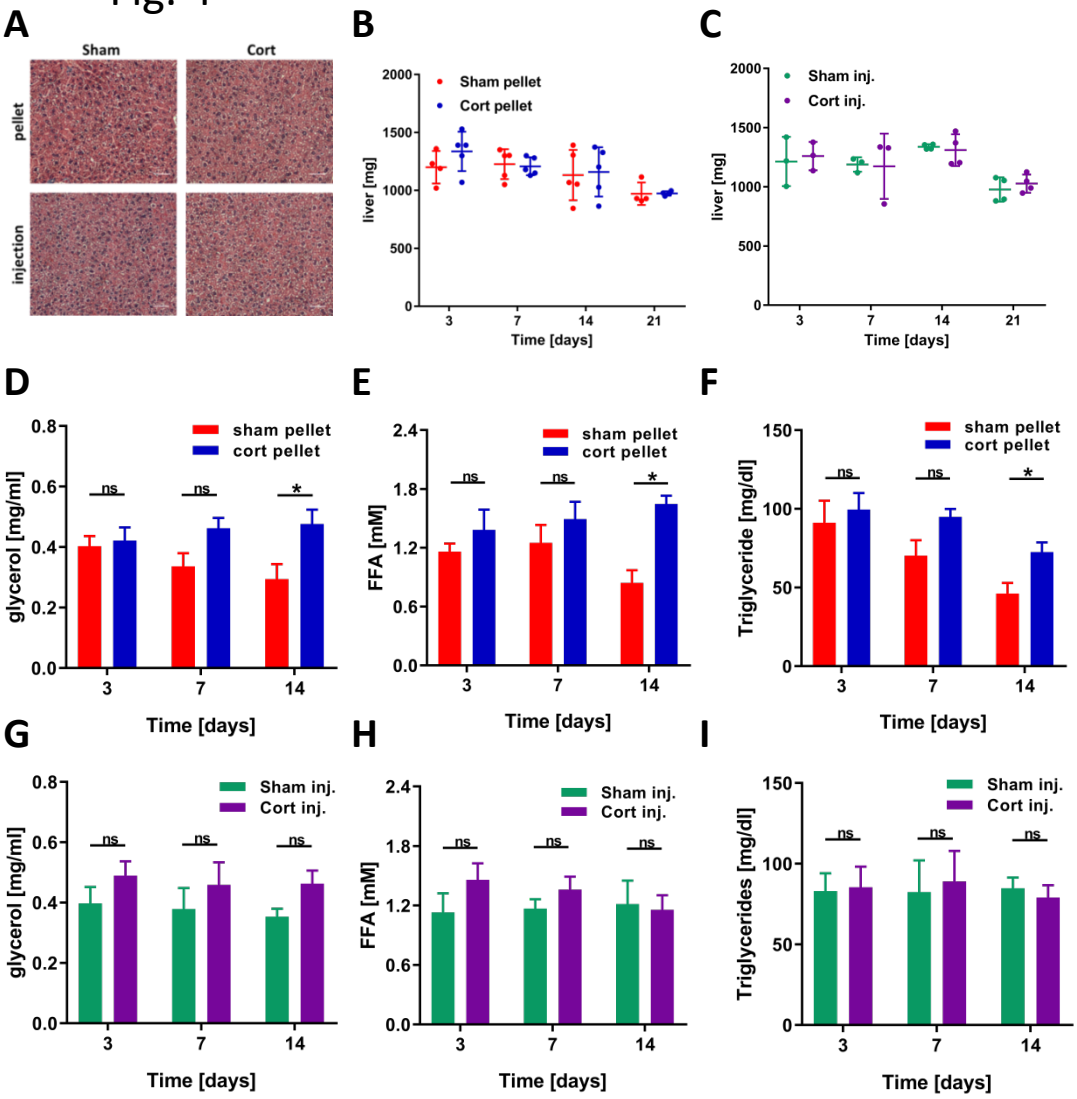

Fig. 5

Tholen et al.

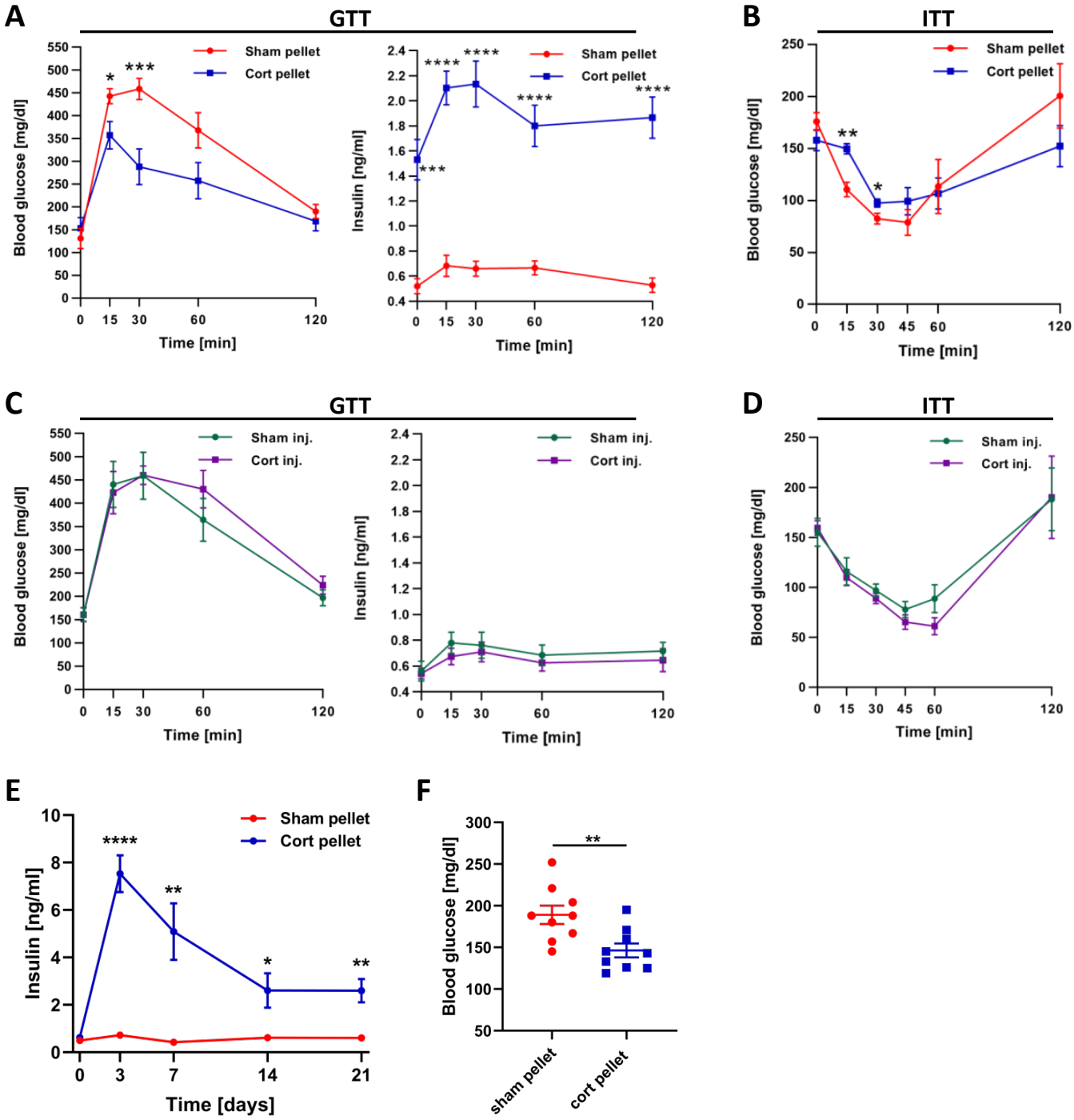

Fig. 6

Tholen et al.

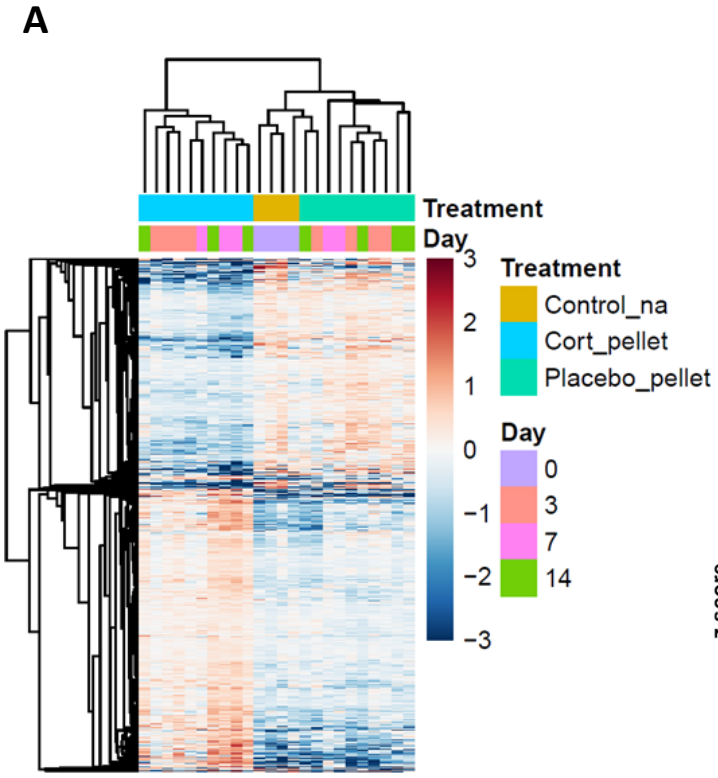

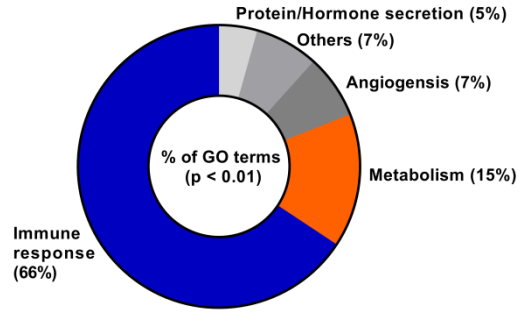

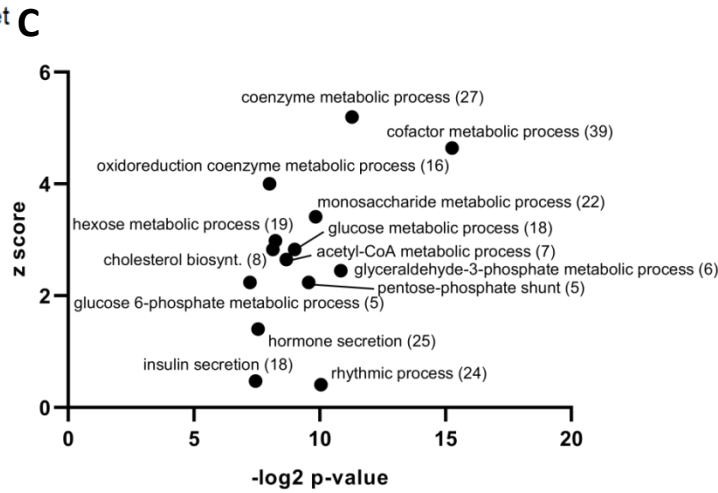

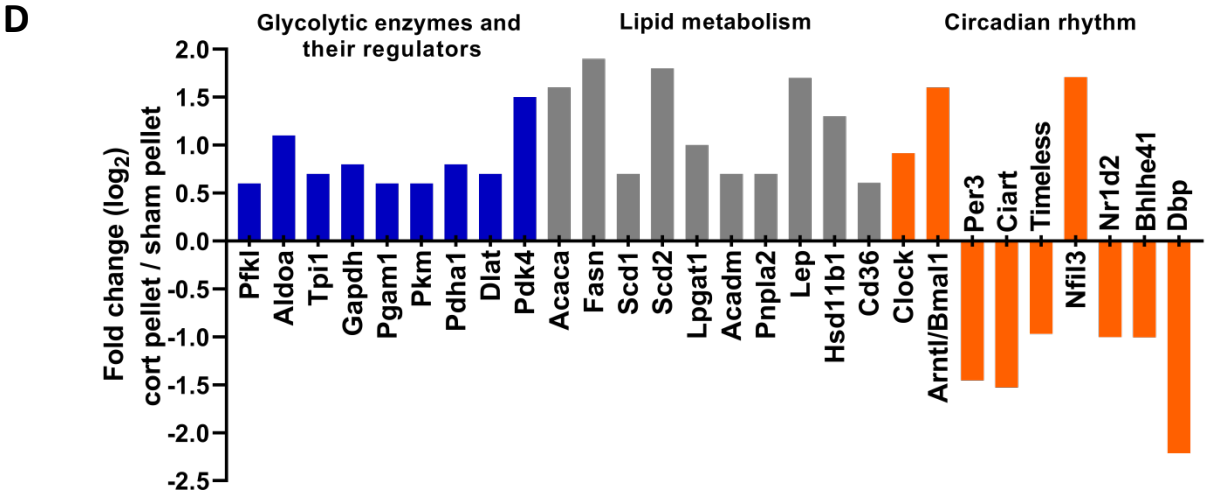

Fig. 7

Tholen et al.

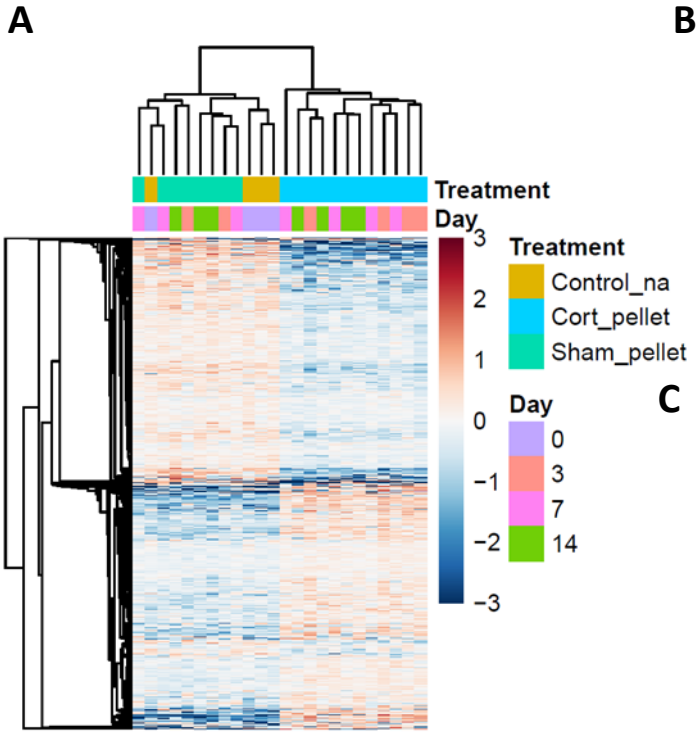

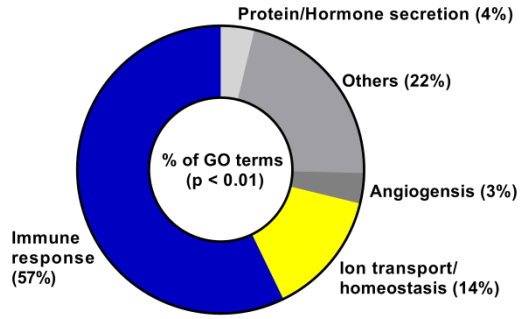

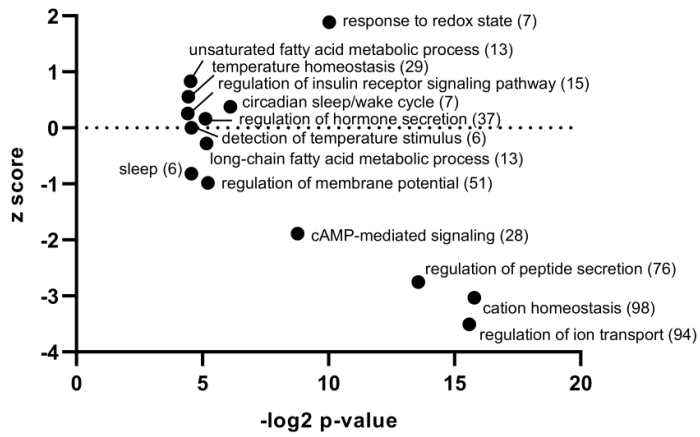

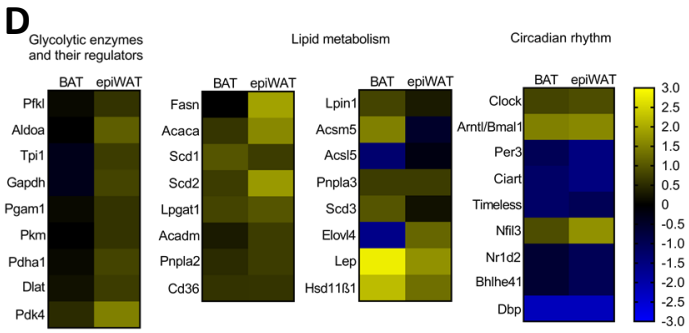

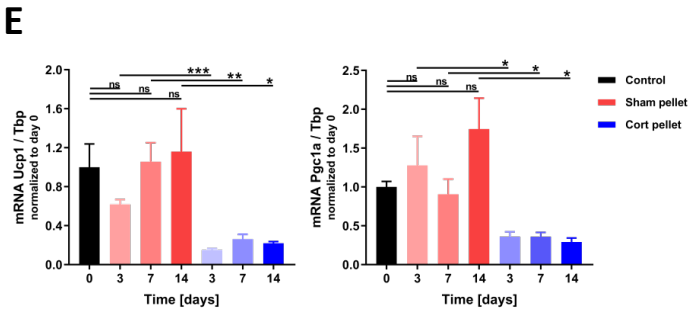

Fig. 8
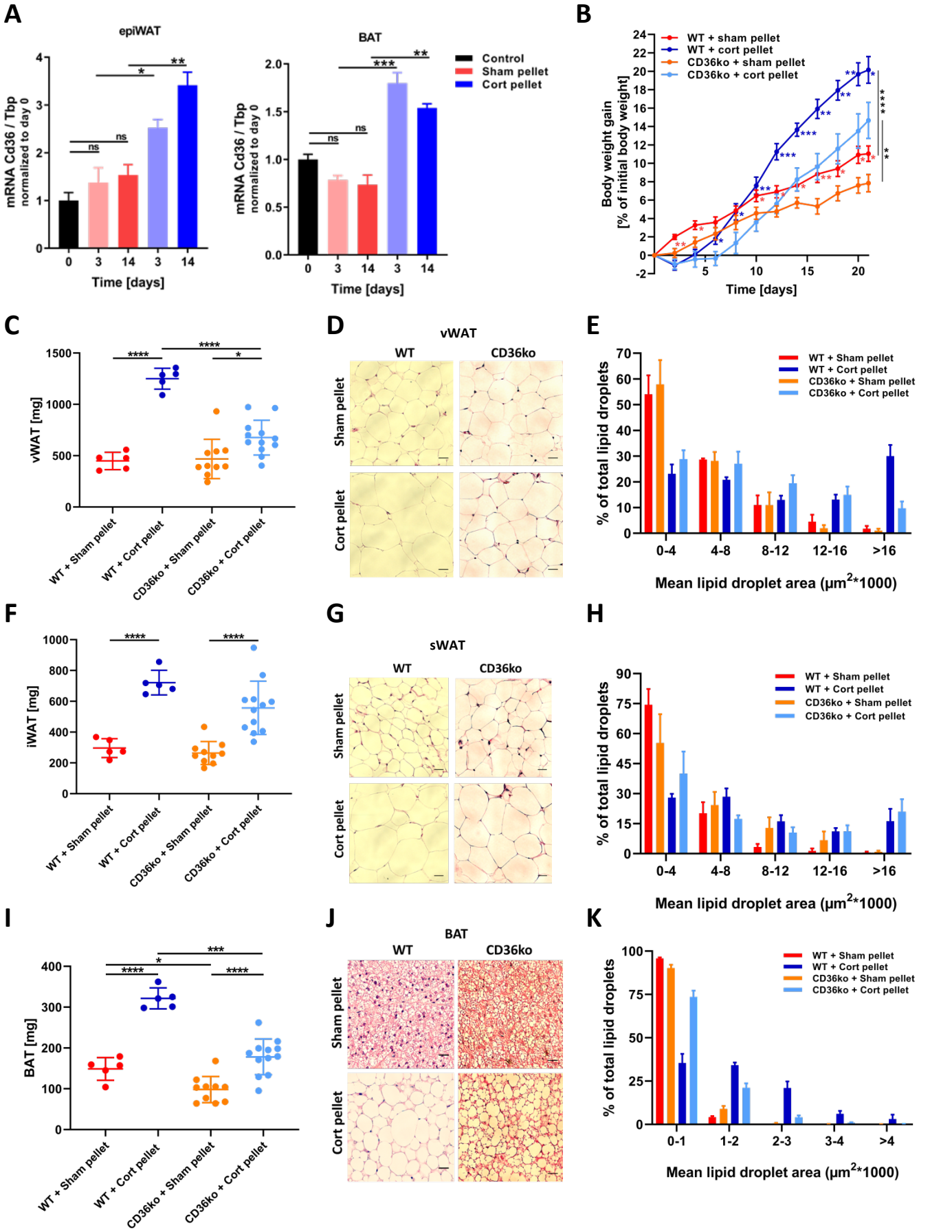
Tholen et al.